# Biological Membranes

## *A Molecular Perspective from Computation and Experiment*

Kenneth M. Merz, Jr. and Benoît Roux
*Editors*

Birkhäuser
Boston • Basel • Berlin

Kenneth M. Merz, Jr.
Department of Chemistry
Pennsylvania State University
152 Davey Laboratory
University Park, PA 16802
USA

Benoît Roux
Groupe de Recherche en Transport
Membranaire (GRTM)
Départements de physique et de chimie
Université de Montréal
C.P. 6128, succ. Centre-Ville
Montréal, Québec
Canada H3C 3J7

**Library of Congress Cataloging-In-Publication Data**

Biological membranes : a molecular perspective from computation and experiment / Kenneth M. Merz, Jr., and Benoît Roux, editors.
p. cm.
Includes bibliographical references and index.
ISBN 0-8176-3827-X (hardcover : acid free). -- ISBN 3-7643-3827-X (hardcover : acid free)
1. Membranes (Biology) 2. Lipid membranes. 3. Membrane lipids. 4. Membrane proteins. I. Merz, Kenneth M., 1959– . II. Roux, Benoît, 1958– .
QH601.B485 1996
574.87'5--dc20 95-51668
CIP

Printed on acid-free paper

*Birkhäuser* ®



ISBN 0-8176-3827-X
ISBN 3-7643-3827-X
Cover design by David Gardner, Dorchester, MA.
Typeset by University Graphics, York, PA.
Printed and bound by Braun-Brumfield, Ann Arbor, MI.
Printed in the U.S.A.

9 8 7 6 5 4 3 2 1

# 13

# Thermodynamics of the Interaction of Proteins with Lipid Membranes

THOMAS HEIMBURG AND DEREK MARSH

## Introduction

Peripheral proteins associated at the lipid surface are one of the major components of biological membranes. They may function in situ as electron carriers (e.g., cytochrome *c*), as enzymes (e.g., protein kinase C), as signal transduction proteins (e.g., G-proteins), or primarily as structural elements (e.g., spectrin and myelin basic protein). The protein density at the membrane surface can be relatively high, and the peripheral proteins may also interact with the exposed portions of integral proteins embedded within the membrane (e.g., with redox enzymes of the respiratory chain, or with receptors such as those to which G-proteins are coupled). The association with the membrane is most frequently of electrostatic origin but may also include surface adsorption and hydrophobic components. The interactions of the isolated peripheral proteins with lipid bilayer membranes, therefore, are of direct relevance to the structure and function of biological membranes, and the determination of binding isotherms has proved to be particularly useful in the study of such interactions. Analysis of the latter constitutes the first and an important part of this chapter that is directly relevant to the thermodynamics of binding.

From a biophysical point of view, the binding of peripheral proteins to lipid membranes has a profound influence on parameters such as the electrostatic surface potential or the enthalpy and the heat capacity of the lipid-protein system. These parameters determine the phase transition behavior of lipid membranes as well as the energetics of the binding reaction itself. At temperatures close to a phase transition, the thermodynamic properties of protein binding cannot be considered separately from, for example, the chain-melting reactions. It is evident from calorimetric heat capacity profiles that the chain-melting of

*Biological Membranes*
K. Merz, Jr. and B. Roux, Editors

lipids is influenced by the binding of proteins. As a direct consequence, the binding of proteins must be influenced by changes in the lipid state. Therefore, the change in lipid state shows up in the behavior of binding isotherms of proteins to membranes. Correspondingly, the binding reaction results in shifts, broadening, or enthalpy changes of the calorimetric heat capacity profiles of lipid chain-melting. Also, structural changes in the lipid matrix might occur as a consequence of protein binding due to the change in the overall physical properties of the lipid-protein complex. Consideration of the lipid chain-melting transition, and its coupling to the lipid binding and lipid-protein interactions, from a thermodynamic point of view constitutes the second part of this chapter.

Although most principles described below are generally applicable, in the following we shall restrict the thermodynamic treatment of protein binding at the membrane to extended planar lipid surfaces. A goal of this chapter is to link the thermodynamics of binding with that of chain-melting and to discuss the consequences for protein function. For this, we first outline a general description of the electrostatics of binding as a function of ionic strength and lipid composition with emphasis particularly on binding isotherms for continuous membrane surfaces. We then apply some of the results to the description of the chain-melting reaction in the presence of proteins. It will be shown that changes of the state of the membrane can result in a change of the protein distribution on the surface, as well as in changes in the forces acting on the bound proteins. These changes correlate with functional changes observed in some proteins. We shall discuss several examples for integral and peripheral proteins in which lipid chain-melting and function of the protein are in a clear relation to each other.

## Binding of Peripheral Proteins to Lipid Surfaces

The binding of peripheral proteins to membranes is controlled by a variety of different interactions. Most important are the electrostatic interactions between charges on the bound protein and the individual charges on the lipids. Also of relevance are nonelectrostatic or hydrophobic contributions to the binding introduced by interactions of the protein with the hydrocarbon chains of the membrane lipids. A third important factor is the interaction between proteins bound to the surface which can lead to dimerization or aggregation of individual protein molecules. Furthermore, the degree of binding is affected by the finite size of the proteins, and, in lipid mixtures, the lateral distribution of lipids is very likely to be affected by the specificity of interaction of the various lipids with the proteins. These interactions are, in general, dependent on the degree of binding, particularly because of the special nature of ligand binding to continuous surfaces.

*Binding Isotherms*

The simplest and most frequently used approach to describe ligand binding to surfaces is the Langmuir isotherm. It describes how much of a ligand (protein) is bound to a surface of given size as a function of the free ligand concentration. In this model, the concentrations (or activities) of free ligand $[L]$, occupied binding sites $[S_b]$, and free binding sites $[S_f]$ are related to the binding constant, $K$, by the mass action law:

$$K = \frac{[S_b]}{[S_f] \cdot [L]} \tag{1}$$

which gives rise to the following binding isotherm:

$$[L] = \frac{1}{K} \cdot \frac{\theta}{(1-\theta)} \tag{2}$$

where $\theta = [S_b]/([S_b] + [S_f])$ is the fraction of occupied sites. A model that is compatible with the law of mass action implies the existence of localized, independent binding sites on the membrane surface (see Figure 1, top). In general, this assumption is not appropriate for a lipid membrane because a lipid bilayer represents a continuous surface. Proteins are free to arrange in such a way that the free surface area between two adjacent bound proteins is greater than zero but smaller than a protein cross section. This means that, in the continuous case, the surface accessible for binding is smaller than the total free surface (see Figure 1, bottom). A further aspect is that there might also exist specific attractive or repulsive interactions between ligands bound to the surface which could lead to aggregation, as indicated schematically by the arrows in Figure 1 (bottom).

These features that are specific to the association with continuous surfaces become most important at higher degrees of binding and are often neglected in considering the binding of peripheral proteins to membranes. Because the surface concentration of proteins in natural membranes can be quite high, it is worthwhile to consider these particular aspects specifically here before going on to a more complete and general treatment. It has been found, for instance, that such effects are important in interpreting the displacement of peripheral proteins from the membrane surface at high ionic strength (Heimburg and Marsh, 1995).

The lateral interactions between proteins that control their distribution on the membrane surface give rise to a two-dimensional pressure, $\Pi(i)$, where $i$ is the number of proteins bound. It is therefore convenient, for illustrative purposes, to analyse these in terms of the Gibbs absorption isotherm (Aveyard and Haydon, 1973):

$$\frac{d\Pi(i)}{d\ln[L]} = \frac{ikT}{n\Delta A} \tag{3}$$

where $n$ is the maximum number of proteins that ideally can be accommodated on the surface, $\Delta A$ is the excluded area per protein, and $[L]$ is the free pro-

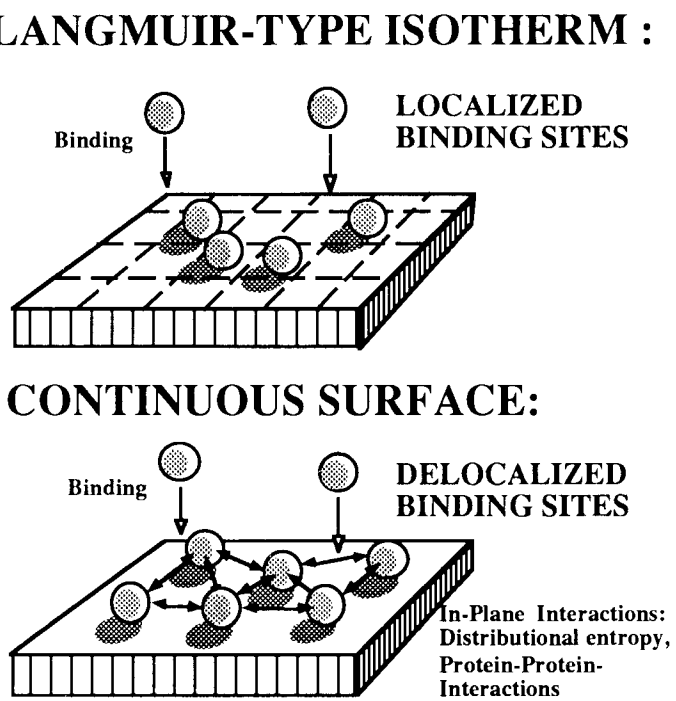


**Figure 1.** Schematic indication of different models for the association of peripheral proteins with membranes. Top: Binding to a surface lattice with fixed independent binding sites, as assumed for the Langmuir isotherm. Bottom: Binding to a continuous surface allowing for in-plane protein rearrangement and protein-protein interaction, indicated by the arrows.

tein concentration (or activity). The simplest expression for the lateral pressure between proteins bound to a continuous surface (i.e., for nonlocalized binding sites) is the Volmer equation of state:

$$\Pi(i) = \frac{ikT}{(n-i)\Delta A}. \tag{4}$$

This equation takes explicit account of the finite size of the protein ligands, but does not include specific interactions between the bound proteins. It is straightforward to show by differentiating Equation 4 with respect to $i$, substituting from Equation 3, and then integrating, that the corresponding isotherm is given by (Haydon and Taylor, 1960):

$$[L] = \frac{1}{K} \cdot \frac{\theta}{1-\theta} \exp\left(\frac{\theta}{1-\theta}\right) \tag{5}$$

where $\theta = i/n$ is the degree of surface coverage and $K$, which is derived from the integration constant, is the effective binding constant. This equation differs by the exponential factor from the standard Langmuir isotherm (Equation 2), which is appropriate for binding to fixed localized sites. The difference arises from the

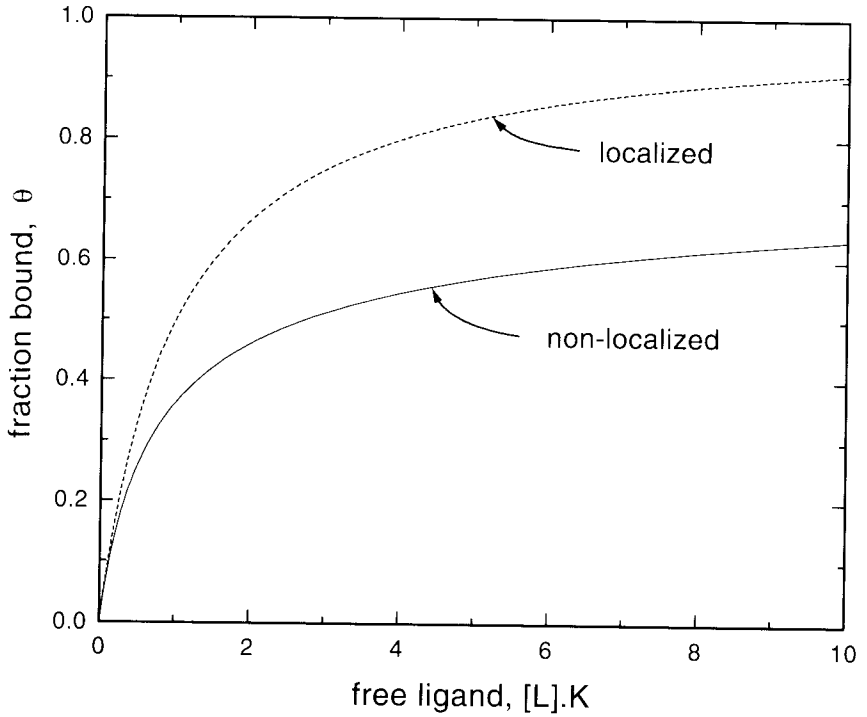


**Figure 2.** Comparison of the binding isotherm for a continuous surface calculated according to Equation 5 (full line) with the Langmuir isotherm (Equation 2) for binding to fixed sites (dashed line). The degree of ligand binding, $\theta$, is plotted as a function of the free ligand concentration, $[L]$, multiplied by the binding constant, $K$.

modification of the distributional entropy for nonlocalized binding to continuous surfaces compared with that to fixed binding sites (Figure 1). The result of this is that, at high concentrations of free ligand, less protein is bound to continuous surfaces (Figure 2). This difference also becomes particularly pronounced for high binding constants. Only at very low degrees of binding ($\theta \ll 1$), for which steric interactions are unimportant, is the binding to continuous surfaces similar to that described by the Langmuir isotherm.

In mixed lipid membranes, the protein additionally can display a preferential affinity for different lipids, e.g., the protein may prefer charged lipids over uncharged lipids. A consequence of this may be a local rearrangement of the lipids to a degree that depends also on the mixing properties of the lipids. Figure 3 shows the three different arrangements that arise if the lipids do not mix at all (bottom), if they distribute according to the relative affinities for the protein (center), or if they mix in a fashion that results in a homogeneous distribution (top). The first case occurs either if unlike lipid species have energetically very unfavorable interactions with unlike nearest neighbor lipids or if the affinity of the protein for one lipid type is extremely high relative to the other lipid

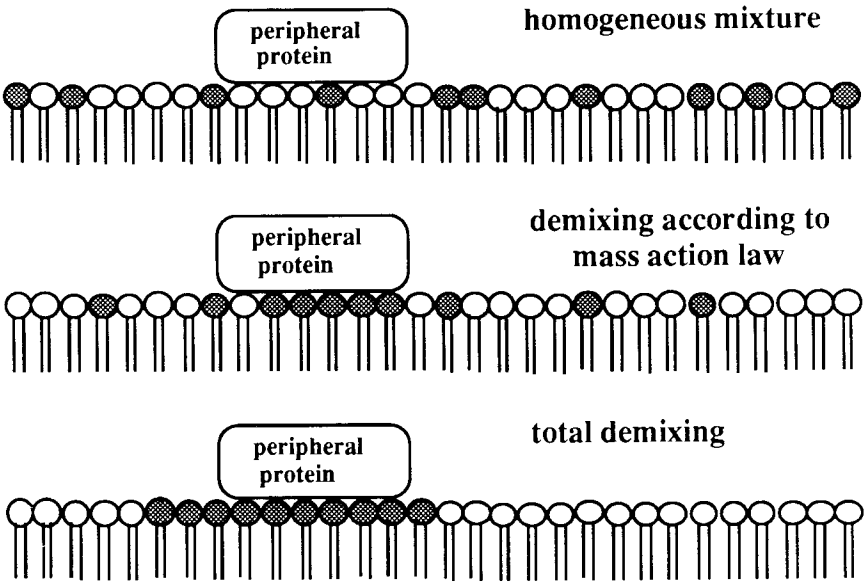


**Figure 3.** Schematic representation of the lipid rearrangement in a mixed lipid membrane upon the binding of peripheral proteins. Top: homogeneous lipid mixture in which no lipid rearrangements take place. Middle: lipids with no preferential interaction which redistribute according to the different affinities for the protein. Bottom: totally unmixed lipids forming in-plane membrane domains.

type. The lipids then either form preexisting domains of different composition to which the protein binds with different affinity or form domains that are induced by the protein binding (Figure 3, bottom). In the case of homogeneous mixtures, the interactions between unlike lipids are favored so strongly that the formation of domains is inhibited even in the presence of proteins (Figure 3, top). In this case, the binding is generally weaker than when domains are formed. In the intermediate case, there are no preferential interactions between lipids and the lipids alone mix statistically. However, for binding of a protein that associates preferentially with one of the lipid species, a local rearrangement of the lipids occurs, which increases the local binding strength (Figure 3, center). In general, different lipid mixing behavior reflects itself in the form of the binding isotherms.

*General Statistical Mechanical Model*

A general way to express the binding is given by the following statistical mechanical expression for the mean number, $\langle i \rangle$, of ligands bound to the membrane (Cantor and Schimmel, 1980):

$$\langle i \rangle = \frac{\sum_{i=1}^{n} i \cdot \frac{1}{i!} K^i [L]^i \exp\left(-\frac{\Delta F(i)}{kT}\right)}{\sum_{i=0}^{n} \frac{1}{i!} K^i [L]^i \exp\left(-\frac{\Delta F(i)}{kT}\right)} \tag{6}$$

where $\Delta F(i)$ is the overall free energy change upon binding $i$ ligands. It is possible to show that this equation can be expressed in the following condensed form (Heimburg and Marsh, 1995):

$$\langle i \rangle = K[L] \exp\left(-\frac{d}{di}\left[\frac{\Delta F(i)}{kT}\right]\right) \tag{7}$$

where $d\Delta(F(i)/di$ is the free energy of binding a single ligand when $i$ ligands are already bound. If the dependence of the free energy change, $\Delta F(i)$, on the number of bound ligands is known, one can then derive the binding isotherms for any specific situation. The free energy change, $\Delta F(i)$, in the case of the Langmuir isotherm is given by the distributional entropy contribution, which is Boltzmann's constant times the logarithm of the number of ways of arranging $i$ ligands on a surface with n sites. This results in $\Delta F(i) = -kTln[n!/(n-i)!]$ for a model with fixed sites. By using Stirling's formula and Equation 7, one can readily verify that this yields the Langmuir isotherm (i.e., Equation 2).

In a protein-membrane complex, the expression for the free energy is more complicated. As well as distributional terms, it also contains contributions from ligand-ligand interactions, from electrostatics, and from redistribution of the different lipids in the membrane plane upon ligand binding. These contributions are designated by $\Delta F_{\text{dist}}(i)$, $\Delta F_{\text{LL}}(i)$, $\Delta F_{\text{el}}(i)$, and $\Delta F_{\text{LD}}(i)$, respectively. The total free energy change with $i$ ligands bound is then:

$$\Delta F(i) = \Delta F_{\text{dist}}(i) + \Delta F_{\text{LL}}(i) + \Delta F_{\text{el}}(i) + \Delta F_{\text{LD}}(i). \tag{8}$$

The different terms in this equation are treated separately in the sections following.

### *Distributional Free Energy*

The distributional free energy term, $\Delta F_{\text{dist}}$, has already been considered above. It may be generalized to include the lateral interactions between bound proteins, $\Delta F_{\text{LL}}$, by using an equation of state for the two-dimensional surface pressure, $\Pi(i)$, that explicitly accounts for the ligand-ligand interactions. This combined free energy change is then given by the work done against the surface pressure on bringing the proteins to their equilibrium surface density:

$$\Delta F_{\text{dist}}(i) + \Delta F_{\text{LL}}(i) = -\int \Pi(i) dA \tag{9}$$

where the integration extends from a reference area that corresponds to infinite ligand separation to the area of the membrane. As a first approximation for the lateral interactions, one can take the Van der Waals equation of state for a two-dimensional gas, which includes also the excluded area term:

$$\Pi(i) = \frac{ikT}{(n-i)\Delta A} - a\left(\frac{kT}{\Delta A}\right)\left(\frac{i}{n}\right)^2. \tag{10}$$

Here $a$ is an empirical parameter characterizing the attractive ($a > 0$) or repulsive interactions ($a < 0$) between bound proteins. In the absence of membrane surface electrostatics, this results (from Equations 7 and 8) in the following binding isotherm for a lipid surface (Heimburg and Marsh, 1995):

$$[L] = \frac{1}{K}\frac{\theta}{1-\theta}\exp\left(\frac{\theta}{1-\theta} - 2a\theta\right) \tag{11}$$

where the integration reference state from Equation 9 is absorbed into the binding constant, K. This isotherm is identical to the isotherm obtained previously by Hill (1946) by using other means, and differs from that derived from the Volmer equation of state (Equation 5) by inclusion of the interaction term.

*Electrostatic Free Energy*

Now we consider the binding of a charged ligand to a lipid membrane in the presence of surface electrostatics. The electrostatic interaction of ligands with surfaces depends on the number of charges involved in the binding reaction. It is assumed that each surface binding region for a protein corresponds to $\alpha$ lipid molecules of which a fraction $f$ are charged, and that each protein ligand bears $Z$ net charges of opposite sign. The change in electrostatic free energy, $\Delta F_{el}(i)$, is given by the difference between the electrostatic free energy of the system before and after binding:

$$\Delta F_{el}(i) = F_{el}^{S}(i) - F_{el}^{S}(0) - i \cdot F_{el}^{L} \tag{12}$$

where the first two terms on the right-hand side represent the surface electrostatic free energy and the last term that of the free ligand in the bulk medium. By using Gouy-Chapman double-layer theory to obtain the electrostatic free energy of the surface (Jähnig, 1976) and Debye-Hückel theory for the electrostatic self energy of the free ligand (Tanford, 1955), one then can obtain an analytical expression for the change in total electrostatic free energy on binding of the charged ligand.

In the high potential limit, the electrostatic free energy of a surface, $F_{el}^{S}$, derived from standard electrostatic double-layer theory, is given by (Jähnig, 1976):

$$F_{el}^{S} = -2q \cdot \left(\frac{kT}{e}\right) \cdot \ln\left(-\frac{\Lambda_0 \sigma}{\sqrt{c}}\right) \tag{13}$$

where $\Lambda_0 = (1000\pi/2\varepsilon N_A kT)^{1/2}$ is a constant, $\sigma$ is the surface charge density, $q$ is the total surface charge, and $c$ is the ionic strength of the (assumed) monovalent salt, $e$ is the elementary charge, and $N_A$ is Avogadro's number. For a surface of total area equal to $n$ protein cross sections, with $i$ proteins bound, the total charge, $q$, and the mean charge density, $\sigma$, are given by:

$$q = -(n\alpha f - iZ) \cdot e \tag{14}$$

$$\sigma = -\left(1 - \frac{iZ}{n\alpha f}\right) \cdot \frac{e}{a_0} f \tag{15}$$

where $a_0$ is the area per lipid molecule. It is assumed here that the charged lipids bear a single negative charge, that the proteins are positively charged, and also that charged and uncharged lipids are mixed homogeneously. The implications and the limitations of the latter assumption are discussed later.

A detailed calculation results finally in the following form for the absorption isotherms of charged lipid membranes (Heimburg and Marsh, 1995):

$$[L] = \frac{1}{K(0, f)} \left(1 - \theta \frac{Z}{f \cdot \alpha}\right)^{-2Z} \frac{\theta}{1-\theta} \exp\left(\frac{\theta}{1-\theta} - 2a\theta\right) \tag{16}$$

where $K(0, f)$ is the binding constant for initial ligand binding, i.e., with no appreciable electrostatic neutralization. This initial binding constant has the following dependence on the ionic strength, $c$, provided that the lipid distribution is homogeneous (Heimburg and Marsh, 1995):

$$K(0, f) = K' \cdot c^{-(Z+\Lambda Z^2)} \cdot f^{2 \cdot Z} \tag{17}$$

where $\Lambda = e^2/16\varepsilon r_0 kT$ arises from the electrostatic self energy of the protein ($r_0$ is the protein radius) and is relatively small. Equation 17 results in a linear dependence of the initial binding on ionic strength in a double logarithmic plot, from which the effective charge, $Z$, on the protein and, $K'$, which contains the intrinsic binding constant, $K$, may be determined. Having obtained these constant parameters, the entire binding curves, at different ionic strengths, may then be analyzed by combining Equations 16 and 17.

*Free Energy of Lipid Redistribution in Mixed Lipid Systems*

As discussed earlier, the strength of protein binding to mixed lipid membranes depends on the mixing properties of the component lipids and, in general, on the redistribution of the lipids in response to the protein binding. If the charged and uncharged lipids are mixed homogeneously and remain so on protein binding (Figure 3, top), then the binding isotherm can be described by Equations 16 and 17 above, in which $f$ is the fraction of charged lipid. If, at the other extreme, the charged and uncharged lipids separate completely forming macroscopic domains (Figure 3, bottom), then the protein binds only to the domains consisting of charged lipids. The effective membrane area for binding is correspondingly reduced, but the strength of binding is that characteristic of a bilayer consisting

wholly of charged lipids. In this case, the binding isotherm can be described again by Equations 16 and 17, but with the replacements $f \rightarrow 1$ and $\theta \rightarrow \theta/f$ at all occurrences of these quantities.

Protein binding to most real mixed lipid membranes generally shows a behavior intermediate between these two limiting cases described above. If there are no preferential interactions between any of the lipids, then the binding of charged proteins tends to recruit the lipids of opposite charge into the vicinity of the protein binding site (Figure 3, middle). The energetic effects of this lipid redistribution are represented by the contribution, $\Delta F_{\mathrm{LD}}(i)$, to the total free energy in Equation 8. To determine this term, the binding can be split into two consecutive steps: an absorption to a homogeneously charged surface as described above and an additional lipid redistribution step, arising from the local binding properties. As an approximation, the latter can be described by an in-plane multiple binding reaction according to the mass action law (Cutsforth et al, 1989). Adopting this approach, the resultant protein binding constant is $K_{eff} = K(0, f)(1 + K_s f_i)^{\alpha}$, and the free energy of binding the charged lipids in the redistribution process is given by (Cutsforth et al, 1989):

$$\Delta F_{\mathrm{LD}}(i) = -\alpha kT \ln(1 + K_s f_i) \tag{18}$$

where $K_s$ is the in-plane surface binding constant and $f_i$ is the surface concentration of charged lipid that is unbound when $i$ proteins are associated with the lipid surface. This contribution to the binding isotherm is then given from Equation 7 by the dependence on $i$ of the fraction, $f_i$, of free lipids that are charged.

### *Experimental Binding Isotherms*

As shown in the previous paragraphs, the study of binding isotherms can give information on the energetics of binding, the aggregation of ligands due to ligand-ligand interactions, and the mixing of lipids in systems containing more than one lipid species. These aspects are illustrated in the following subsections by experimental results on the binding of the peripheral protein cytochrome *c* to anionic lipids and their mixtures with zwitterionic lipids.

### CYTOCHROME *c* BINDING TO NEGATIVELY CHARGED LIPID MEMBRANES

Binding of cytochrome *c* to charged lipid surfaces leads to a reduction in the protein denaturation temperature. Therefore, one can study the surface binding of both native and denatured forms with the protein still native in solution. This is done by choosing temperatures below and above that for surface denaturation, respectively, with both below that for denaturation of the free protein. Denatured cytochrome *c* tends to aggregate on surfaces. By comparing the native and denatured forms, one can determine the effects of surface ligand-ligand interactions on the binding isotherms.

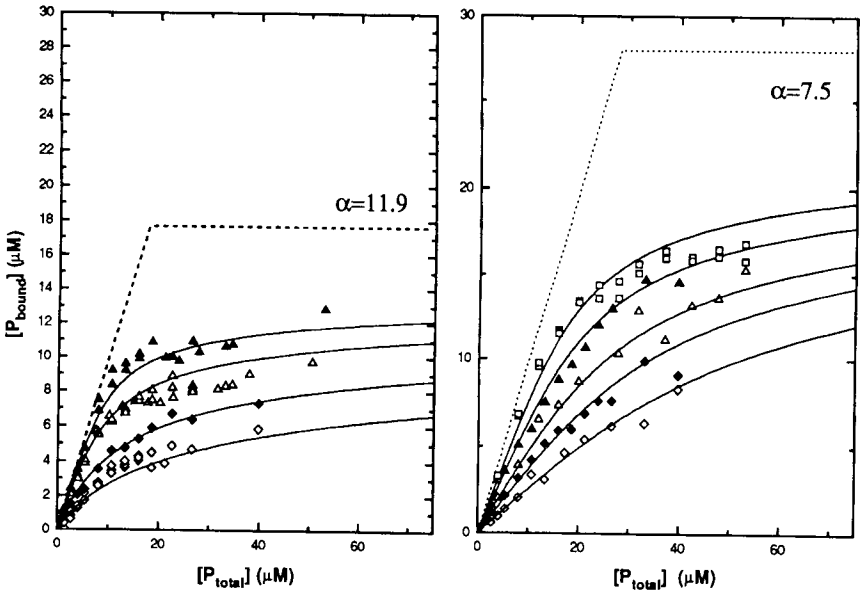


**Figure 4.** Binding isotherms for cytochrome *c* with dioleoyl phosphatidylglycerol membranes at neutral pH and different ionic strengths. Left: Native cytochrome *c* ($T = 20^{\circ}$C) at ionic strengths of 41.9, 54.4, 79.4, and 104.4 mM (from top to bottom) . Solid lines represent a global fit of the isotherms at different ionic strengths to Equation 16 without protein-protein interactions. Right: Surface-denatured cytochrome *c* ($T = 65^{\circ}$C) at ionic strengths of 104.4, 125, 154.4, 175, and 204.4 mM (from top to bottom). Solid lines represent a global fit of the isotherms at the different ionic strengths to Equation 16 using attractive protein-protein interactions. Data from Heimburg and Marsh (1995).

Examples of experimental isotherms for binding of cytochrome *c* to anionic dioleoyl phosphatidylglycerol membranes are given in Figure 4. The intrinsic binding constant $K = 1.9 \times 10^{-5}$ l/mole lipid and the effective charge $Z = +3.8$ for native cytochrome *c* are determined from Equation 17 by measuring the binding at very low degrees of surface coverage. Using these parameters, consistent fits of the isotherms in Figure 4 (left panel) at different ionic strengths to Equation 16 yield a lipid stoichiometry of $\alpha = 11.9$ per protein with the parameter, $a$, for the protein-protein interactions being close to zero. This means that the cross-section of the protein is equivalent to that of 12 lipids in a fluid bilayer which correlates reasonably well with crystallographic data for cytochrome *c* (Dickerson et al, 1971). Also, the binding isotherms indicate that there are few energetically significant interactions between the bound native proteins on the surface, other than steric exclusion (i.e., $a = 0$). The effective charge on the protein is considerably lower than the physical net charge of the protein of +7, including the heme charge, as deduced from the amino acid sequence (Cheddar and Tollin, 1994). Possible reasons for this low effective charge, which is found relatively frequently in the binding of extended multiply charged ligands, have been discussed previously (Heimburg and Marsh, 1995).

An interesting feature of the isotherms in Figure 4 (left panel) is the tendency to flatten off at values well below that corresponding to maximum surface coverage. This tendency becomes more pronounced with increasing ionic strength and is the basis for the removal of peripheral proteins from membranes by washing in high salt. The origin of this effect lies in the nature of binding to continuous surfaces. As the electrostatic component of the binding becomes weaker at high ionic strength, the effective lateral surface pressure between the surface-associated proteins still remains equally effective in preventing further binding (Equations 2 and 5 and Figure 2).

The situation is somewhat different for the binding of surface-denatured cytochrome *c* (Figure 4, right panel). The effective charge on the protein $Z = +3.3$, obtained from the initial parts of the binding isotherms, is similar to that for the native protein, but the intrinsic binding constant $K = 1.6 \times 10^{-3}$ l/mole lipid is considerably larger, corresponding to an increase in binding free energy by approximately −2.5 kcal/mol. For surface-denatured cytochrome *c*, the entire binding isotherms at different ionic strengths only can be fit with a nonzero value for the protein-protein interaction parameter. Global fits to the isotherms yield a reduced stoichiometry of $\alpha = 7.5$ lipids per protein, and a positive interaction parameter of $a = +2.3$. This indicates both that the protein decreases its cross-section on surface denaturation and that at the same time attractive interactions occur between the bound proteins, reflecting a tendency for the denatured proteins to aggregate on the lipid surface. There is independent evidence suggesting aggregation of surface-denatured cytochrome *c* from infrared spectroscopic studies (Heimburg and Marsh, 1993; Muga et al, 1991).

Qualitatively, the effects of the surface aggregation of the denatured cytochrome *c* are seen from comparison of the binding isotherms with those of the native protein in Figure 4. The isotherms for the surface-denatured protein are mostly at higher ionic strength than those given for the native protein. However, for comparable initial binding strengths, the isotherms for the denatured protein display less tendency to flatten off than do those for the native protein. This is because the attractive interactions between the surface-denatured proteins decrease the effective lateral pressure exerted between them, hence allowing more protein to bind.

### CYTOCHROME *c* BINDING TO MIXTURES OF CHARGED AND ZWITTERIONIC LIPIDS

For electrostatic reasons, the admixture with zwitterionic lipids decreases the strength of binding of peripheral proteins to negatively charged lipids. As discussed above, the extent of this effect can differ depending on the mixing properties of the lipids. This is illustrated in Figure 5, which gives the binding isotherm for native cytochrome *c* to a mixed membrane composed of dioleoyl phosphatidylglycerol (60 mol %) and dioleoyl phosphatidylcholine (40 mol %). The experimental binding isotherm is compared with theoretical pre-

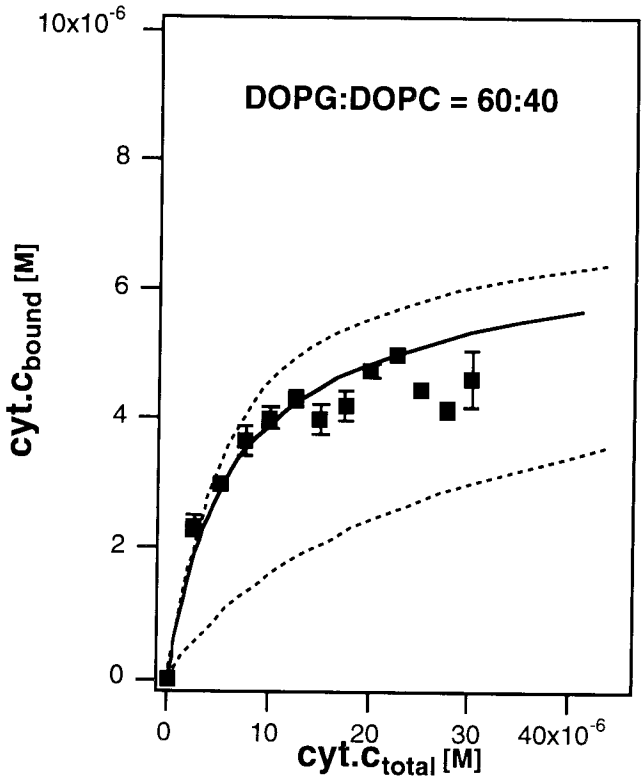


**Figure 5.** Binding isotherm of native cytochrome *c* with mixed lipid membranes composed of dioleoyl phosphatidylglycerol (60 mol %) and dioleoyl phosphatidylcholine (40 mol %) at an ionic strength of 45 mM. The dashed lines correspond to isotherms predicted from Equation 16 for a homogeneous lipid mixture (lower) and for complete separation of the two lipids (upper), using parameters obtained from fitting the data in Figure 4 (left panel). The full line represents a fit to the experimental data that takes into account the redistribution of the lipids on protein binding.

dictions (dashed lines) of the isotherms expected for binding to a homogeneous distribution of the two lipids (Figure 3, top) and to completely separated domains of the negatively charged component (Figure 3, bottom). The predicted isotherms are calculated from Equation 16, using the methods described above. The parameters for binding to dioleoyl phosphatidylglycerol are taken from Figure 4 for native cytochrome *c*, and it is assumed that the binding to zwitterionic phosphatidylcholine is negligible (for which there is experimental evidence). The experimental isotherm lies between those predicted for the two extreme cases, indicating that an in-plane redistribution of the negatively charged lipids in response to protein binding (Figure 3, middle) does in fact take place. The binding is weaker than to separated domains of phosphatidylglycerol but is considerably stronger than to a homogeneous lipid mixture. The experimental binding isotherm can be described adequately by taking into account the free

energy of lipid redistribution with a simple mass action formalism as discussed above (Equation 18). This is indicated by the full line in Figure 5, in which the effective surface lipid binding constant, $K_S$, is related directly to the binding constant, $K(0, 1)$, of native cytochrome $c$ to phosphatidylglycerol obtained above (Figure 4), as expected on energetic grounds.

This example illustrates the way in which analysis of the binding isotherms may be used to determine the rearrangements of the lipid distribution on protein binding, to study the selectivity of interaction of lipids with peripheral proteins (Sankaram and Marsh, 1993), and to obtain information on the mixing properties of lipids in bilayers (Figure 3). The latter aspect bears certain similarities to the determination of the activity of negatively charged phosphatidylserine in lipid mixtures by means of the $Ca^{2+}$-binding properties (Huang et al, 1993).

*Difference in Protein Binding to Gel and Fluid Membrane States*

In general, it is to be expected that the strength of binding of peripheral proteins will be dependent not only on the lipid species but also on the state of the lipid, particularly on whether it is in a gel or a fluid phase. Because the area per lipid molecule, $a_0$, increases appreciably at the gel-to-fluid chain-melting transition of lipid bilayers (Cevc and Marsh, 1987), the surface electrostatic free energy will be lower for fluid bilayers than for gel-phase bilayers, and the strength of binding will decrease correspondingly. According to Equations 13–15, in the high potential limit, the electrostatic free energy of the lipid surface in the presence of protein changes on chain-melting by:

$$\delta[\Delta F_{\mathrm{el}}^{S}(i)]^{\mathrm{melting}} = -2q\left(\frac{kT}{e}\right)\ln\left(\frac{\sigma_{\mathrm{fluid}}}{\sigma_{\mathrm{gel}}}\right) = +2(n\alpha f - iZ)kT\ln\left(\frac{a_0^{\mathrm{gel}}}{a_0^{\mathrm{fluid}}}\right) \tag{19}$$

where $\sigma_{\mathrm{gel}}, \sigma_{\mathrm{fluid}}$ are the surface charge densities, and $a_0^{\mathrm{gel}}, a_0^{\mathrm{fluid}}$ are the areas per lipid molecule in gel and fluid phase bilayers, respectively. The difference in electrostatic free energy of binding a protein, $d\Delta F_{\mathrm{el}}^{S}(i)/di$, to the fluid and gel lipid states is then given by (Heimburg and Marsh, 1995):

$$\delta[d\Delta F_{\mathrm{el}}^{S}(i)/di]^{\mathrm{melting}} = -2kTZ\ln\left(\frac{a_0^{\mathrm{gel}}}{a_0^{\mathrm{fluid}}}\right). \tag{20}$$

In the high-potential regime of electrostatic double-layer theory that is used here, this free energy is almost totally entropic (Jähnig, 1976). Assuming an increase in surface area on lipid chain-melting of approximately 30% (Marsh, 1990), the change in electrostatic binding energy amounts to $\approx +1.2$ kcal/mol protein. This would correspond to a decrease in binding constant of the protein by a factor of approximately eight on chain-melting. Expressing the electrostatic surface free energy difference in terms of the number of lipids yields a value of $\approx +100$ cal/mol per lipid, assuming a lipid/protein stoichiometry of $\alpha = 12$ that

is appropriate to native cytochrome *c*. Energetically speaking, this is a relatively small change, but because of the highly cooperative nature of lipid chain-melting it is capable of changing the gel-fluid equilibrium. The partial neutralization of the membrane electrostatic charge by binding the protein results in a shift in the lipid transition to higher temperatures by an amount that, from perturbation theory for first-order transitions, is given by (Cevc and Marsh, 1987):

$$\Delta T_t = \frac{\delta[d\Delta F_{\mathrm{el}}^{S}(i)/di]^{\mathrm{melting}}}{\alpha \Delta S_t} \tag{21}$$

where $\Delta S_t$ is the chain-melting entropy. Taking a value for the latter of $\approx 23$ cal/mol/K appropriate to dimyristoyl phosphatidylgylcerol (Marsh, 1990) results in an upward shift in transition temperature of $\approx +4$–$5^{\circ}$C. This illustrates the coupling of the lipid chain-melting equilibrium with the protein binding equilibrium via the reciprocal influence of protein binding and membrane surface electrostatics on one another.

Irrespective of mechanism, the different strength of binding of peripheral proteins to different states of the lipid results quite generally in a direct coupling between the lipid-protein interaction and the lipid phase transition. The overall combined association and phase equilibria at fixed temperature can be depicted by the following scheme (Heimburg and Biltonen, 1996):

$$\begin{array}{ccc} & \overset{K^L}{\rightleftharpoons} & \\ P + G & & P + F \\ K_G \quad \uparrow\downarrow & & \uparrow\downarrow \quad K_F \\ P \cdot G & \underset{K^{LP}}{\rightleftharpoons} & P \cdot F \end{array}$$

where $K_G$ and $K_F$ are the association constants of the protein ($P$) with fluid ($F$) and gel ($G$) phase lipids. The apparent equilibrium constants for the gel-fluid equilibria of the free and protein-bound lipid are $K_L = \theta^L/(1-\theta^L)$ and $K^{LP} = \theta^{LP}/(1-\theta^{LP})$, respectively. From the cyclic nature of the equilibria (i.e., $K_G \cdot K^{LP} = K^L \cdot K_F$), the degree of conversion to the fluid phase for the protein-bound lipid ($\theta^{LP}$) is related to that for the free lipid ($\theta^L$) by:

$$\theta^{LP} = r\theta^L/[1 + (r-1)\theta^L] \tag{22}$$

where $r = K_F/K_G$ is the ratio of the association constants with the fluid- and gel-state lipids. This general relation demonstrates that both the mid-point of the transition will be shifted and the shape of the transition curve will be skewed, in the presence of bound protein. In particular, the transition mid-point ($\theta^{LP} = 0.5$) occurs at a temperature for which the degree of transition of the free lipid is: $\theta^L = 1/(r+1)$, which results in downward shifts for $r < 1$ and upward shifts for $r > 1$.

To illustrate simply the effects of protein binding on the gel-fluid lipid coexistence, the cooperativity of the phase transition can be depicted by a one-

dimensional two-state Ising model (Marsh et al, 1976). The degree of transition of the free lipid is then approximated by (Zimm and Bragg, 1959):

$$\theta^L = \frac{1}{2}\left[1 + \frac{s-1}{\sqrt{(s-1)^2 + 4\sigma_L s}}\right] \tag{23}$$

where $s$ is a scaled temperature parameter, and the cooperativity parameter, $\sigma_L$, is determined by the boundary free energy between gel and fluid lipid domains. The transition curves for the protein-bound lipid deduced from Equations (22) and (23) are given for various values of the ratio of fluid and gel association constants in Figure 6. The transition curve for $r = 1$ is identical with that for the free lipid. An increasing preference of the protein for binding to one of the states of the lipid results in a progressive broadening and shift of the transition towards the side of transition that favors the other phase. Under these conditions, the range of phase coexistence is broadened, and the domains of the lipid phase

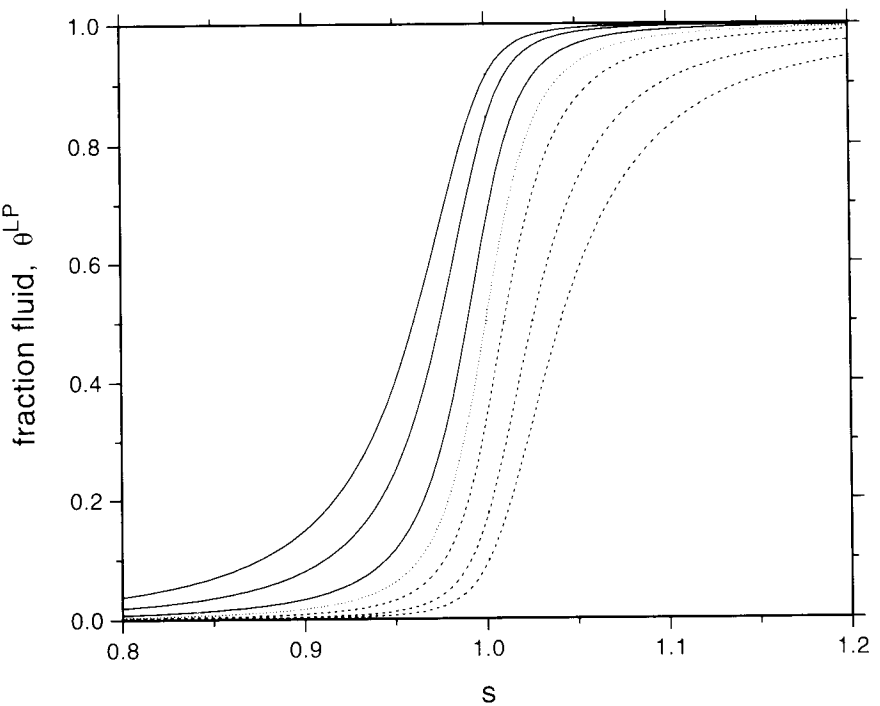


**Figure 6.** Chain-melting transition curves for lipids with bound peripheral protein and various ratios of the protein association constants with gel and fluid lipid. The degree of transition, $\theta^{LP}$, is obtained from Equations 20 and 21 with $\sigma_L = 2.10^{-4}$ and from left to right: $r = 0.1, 0.2, 0.5, 1.0, 2.0, 5.0, 10.0$. The $x$-axis is the dimensionless temperature parameter, $s \approx 1 + (\Delta H_t / RT_t^2)(T - T_t)$, where $T_t$ is the transition temperature of the free lipid (i.e., $s = 1$) and $\Delta H_t$ the corresponding transition enthalpy (Marsh, 1995b).

favoring protein binding are preferentially stabilized. This inevitably gives rise to a nonhomogeneous distribution of protein molecules on the membrane surface, as will be seen in detail later.

## Lipid Chain-Melting and Lipid-Protein Interaction

In the following sections, the lipid chain-melting phase transition and its reciprocal coupling with protein binding and lipid-protein interactions are considered in some detail. The emphasis here is on the formation of spatially separated domains of lipids in the gel and fluid states, and on the ensuing spatial heterogeneity of the in-plane distribution of the membrane-bound proteins. For this purpose, a two-state model (i.e., gel and fluid) is adopted for the lipid phase transition in which only interactions between nearest-neighbor lipids are considered, i.e., a two-dimensional Ising model. In such a model, cooperativity arises in the phase transition because of energetically unfavorable interactions between lipids in different states, which are located principally at the boundaries of the domains composed of lipids in a single state. Monte Carlo calculations based on a fixed two-dimensional lipid lattice are used in order to allow for the entropy of the domain boundaries in a proper manner and at the same time to give direct information on the spatial extent of the domains and their fluctuations. The distribution of proteins bound to the membrane surface is also obtained by the same method.

### *Lipid Transitions and Lipid Domain Formation*

First we consider the chain-melting transition of lipid membranes in the absence of proteins. This is a highly cooperative process with a transition half-width that can be as small as 0.07 degrees (Albon and Sturtevant, 1978). Cooperativity implies that the lipid chains do not melt independently; instead the state of a lipid is dependent on that of the surrounding lipids. In the following it is assumed that interactions take place only between nearest-neighbor lipids that are in one of two states (gel or fluid), i.e., a two-dimensional Ising model.

The nearest-neighbor lipid-lipid interaction free energies are designated by $\varepsilon_{gg}$, $\varepsilon_{ll}$, and $\varepsilon_{gl}$, corresponding to the interaction between two gel lipids, two fluid lipids, and a gel and a fluid lipid, respectively. At temperature $T$, the chain-melting free energy of the bilayer in a particular configuration, for which the number of lipids in the fluid state is $n_l$ and the number of unlike lipid contacts is $n_{gl}$, is then given by:

$$\Delta G(T) = n_l(\Delta H_t - T\Delta S_t) + \frac{1}{2} n_{gl}\omega_{gl} \tag{24}$$

where $\Delta H_t$ and $\Delta S_t$ are the total transition enthalpy and entropy, respectively, and $\omega_{gl} = \varepsilon_{gl} - (\varepsilon_{gg} + \varepsilon_{ll})/2$ is the excess interaction free energy of a pair of

unlike lipids. The mid-point of the transition (strictly speaking, the isoenergetic point) is given by $\Delta G(T) = 0$, and occurs at a temperature $T_m = \Delta H_t / \Delta S_t$, ignoring the small term of order $(n_{gl}/n_l)\omega_{gl}$.

The mean value for any observable, $\langle X \rangle$, can be obtained by averaging over all bilayer configurations at a particular temperature, using the statistical thermodynamic expression:

$$\langle X(T) \rangle = \sum_{n_l} \sum_{n_{gl}} X(n_l, n_{gl}) \cdot P(T, n_l, n_{gl})$$

$$= \frac{\sum_{n_l} \sum_{n_{gl}} X(n_l, n_{gl}) \cdot \Omega(n_l, n_{gl}) \exp\left( -\dfrac{n_l \cdot (\Delta H_t - T\Delta S_t) + \frac{1}{2} n_{gl} \omega_{gl}}{RT} \right)}{\sum_{n_l} \sum_{n_{gl}} \Omega(n_l, n_{gl}) \exp\left( -\dfrac{n_l \cdot (\Delta H_t - T\Delta S_t) + \frac{1}{2} n_{gl} \omega_{gl}}{RT} \right)} \tag{25}$$

where $P(T, n_l, n_{gl})$ is the probability at temperature $T$ of finding a bilayer configuration with a given fraction of lipids in the fluid state and of gel-fluid contacts, and $\Omega(n_l, n_{gl})$ is the number of independent ways of generating such a configuration (i.e., the degeneracy). Possible observables are, for example, the enthalpy, $\langle H \rangle$ or $\langle H^2 \rangle$, or the mean surface area of the bilayer, $\langle A \rangle$. Of particular interest is the mean fraction of fluid lipids, $\langle f \rangle$, where $f = n_l/n$ for a bilayer composed of $n$ lipids.

The main problem in calculating the configurational partition function and the mean value of an observable lies in the determination of the distribution function $\Omega(n_l, n_{gl})$. Because an analytical method is not available, Monte Carlo simulations are used. The simulations are performed numerically by defining a lipid matrix and switching the state of each individual lipid according to the statistical mechanical probability for such a change. If this probability is greater than a randomly generated probability, it is accepted, and if below this value, it is rejected. The relevant probability for an individual lipid to change from the gel state to the fluid state is given by:

$$P = \frac{K(T)}{1 + K(T)} \tag{26}$$

where the statistical weight is given by:

$$K(T) = \exp\left( -\frac{\Delta H_t - T\Delta S_t + \Delta n_{gl} \cdot \omega_{gl}}{RT} \right). \tag{27}$$

Here $\Delta n_{gl}$ is the increase in the number of unlike nearest neighbors upon the change from the gel to the fluid state, where for lipids on a triangular lattice: $-6 \leq \Delta n_{gl} \leq 6$ (see Figure 7). For further details see Mouritsen and Biltonen (1992), Sugar et al (1994) and Heimburg and Biltonen (1996). The Monte Carlo steps are repeated many times so that the distribution function $\Omega(n_l, n_{gl})$ can be determined by counting the relative numbers of the respective configurations generated. The Metropolis procedure used for obtaining $\Omega(n_l, n_{gl})$ can be described as a representative random walk through the phase space and is

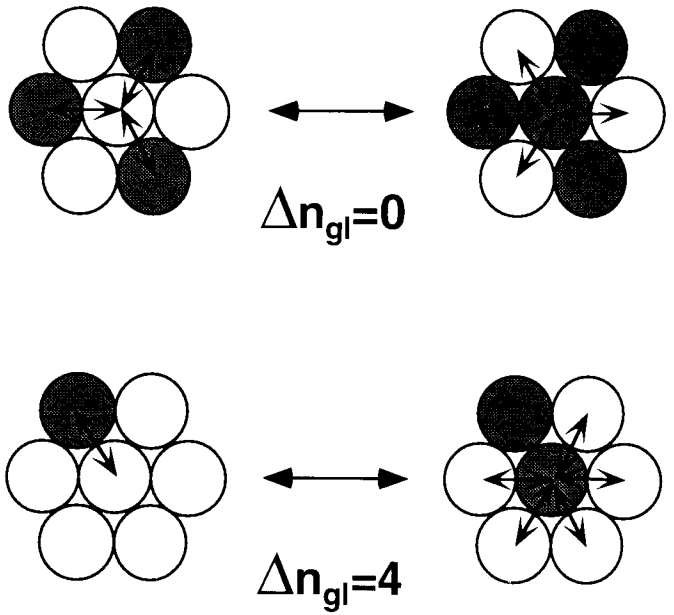


**Figure 7.** Illustration of the change in state of a lipid during a Monte Carlo step. The lipids are arranged on a triangular (i.e., centered hexagonal) lattice, and gel-state and fluid-state lipids are depicted by open and shaded circles, respectively. Two cases are given in which the number of unlike nearest-neighbors of the central test lipid changes by $\Delta n_{gl} = 0$ and $\Delta n_{gl} = 4$. In general: $\Delta n_{gl} = z - 2n_{gl}$, where $z$ is the total number of nearest-neighbors (i.e., the coordination number) and $n_{gl}$ is the original number of unlike nearest-neighbors before the change of state (Heimburg and Biltonen, 1996).

required to be performed only once. When the distribution $\Omega(n_f, n_{gl})$ is known, the mean value of an observable $\langle X \rangle$ can be derived for any given set of values for the parameters $\omega_{gl}$, $\Delta H_f$ and $\Delta S_f$, and at a particular temperature $T$, by using Equation 25 (Ferrenberg and Swendson, 1988).

By differentiating Equation 25 for $\langle H \rangle$ with respect to temperature, the molar heat capacity at constant pressure, $C_p$, can be determined, yielding the well-known fluctuation-dissipation theorem from statistical mechanics (Hill, 1960):

$$C_p = \left( \frac{\partial \langle H \rangle}{\partial T} \right)_p = \frac{\langle H^2 \rangle - \langle H \rangle^2}{RT^2}. \tag{28}$$

The required averages, $\langle H^2 \rangle$ and $\langle H \rangle$, are obtained from Equation 25. In the two-state model, each is related to the corresponding mean values for the fraction of fluid lipids, $f$, i.e.:

$$C_p = [\langle f^2 \rangle - \langle f \rangle^2] \frac{(\Delta H_f)^2}{RT^2} \tag{29}$$

because the molar chain-melting enthalpy at fluid fraction $f$ is given simply by: $\Delta H(f) = f \Delta H_f$. This latter holds as long as the enthalpic contribution

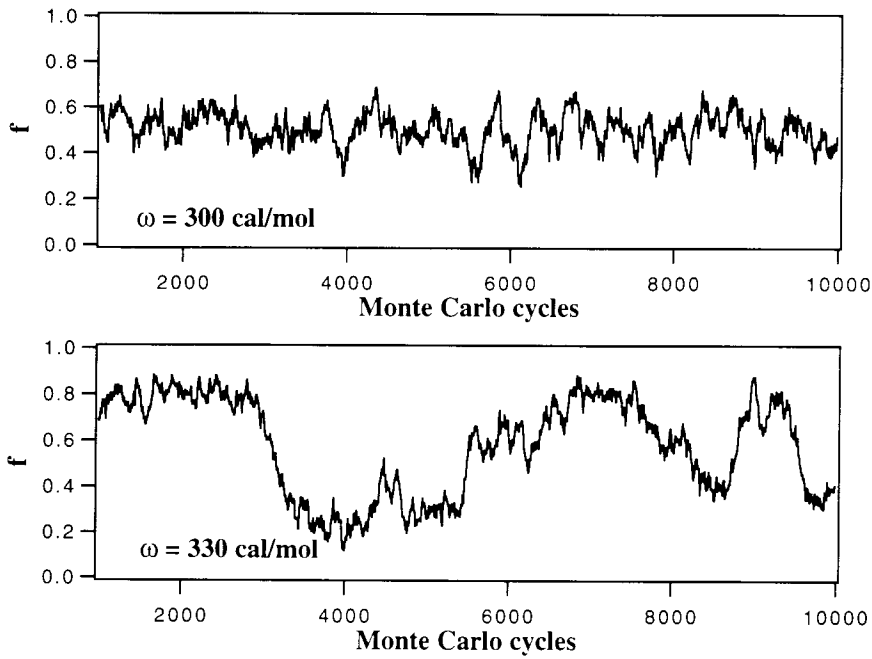


**Figure 8.** Fluctuations in the percentage of fluid lipids about a mean value of 50% obtained over a range of 9000 Monte Carlo cycles with a 41 × 41 lipid matrix. The initial 1000 simulation steps were discarded in order to ensure that a representative configuration had been achieved. The parameters used for the simulation were $\Delta H_t = 8.7$ kcal/mol, $\Delta S_t = 28$ cal/mol/K, and an enthalpic interaction energy of $\omega_{gl} = 300$ cal/mol (upper) or 330 cal/mol (lower) with a triangular lattice and a temperature corresponding to the mid-point of the gel-to-fluid transition of $T_m = 310.3$ K.

from the interfacial free energy, $\omega_{gl}$, which is relatively small, can be neglected. From the properties of mean values, it can readily be shown that $\langle f^2 \rangle - \langle f \rangle^2 = \langle (f - \langle f \rangle)^2 \rangle$, i.e., that the quantities of interest are the mean-square fluctuations about the mean value.

The fluctuations in the fraction of fluid lipids obtained from a Monte Carlo simulation for lipids on a triangular lattice are illustrated in Figure 8. The temperature chosen for the simulation corresponds to the mid-point of the gel-to-fluid bilayer transition, and, therefore, the fluctuations about the mean value of 50% are especially large. Simulations are given for two values of $\omega_{gl}$; for the moment we concentrate on the upper one corresponding to the lower degree of cooperativity. This simulation allows the calculation of the heat capacity maximum $C_p^{\max}$ for the transition, by using Equation 29. Having established the relevant parts of the distribution function, $\Omega(n_l, n_{gl})$, in this way by a single simulation, it is then possible to calculate the heat capacity profile as a function of temperature from Equation 25. The results for various values of the interfacial free energy parameter, $\omega_{gl}$, are given in Figure 9. It can be seen that increasing

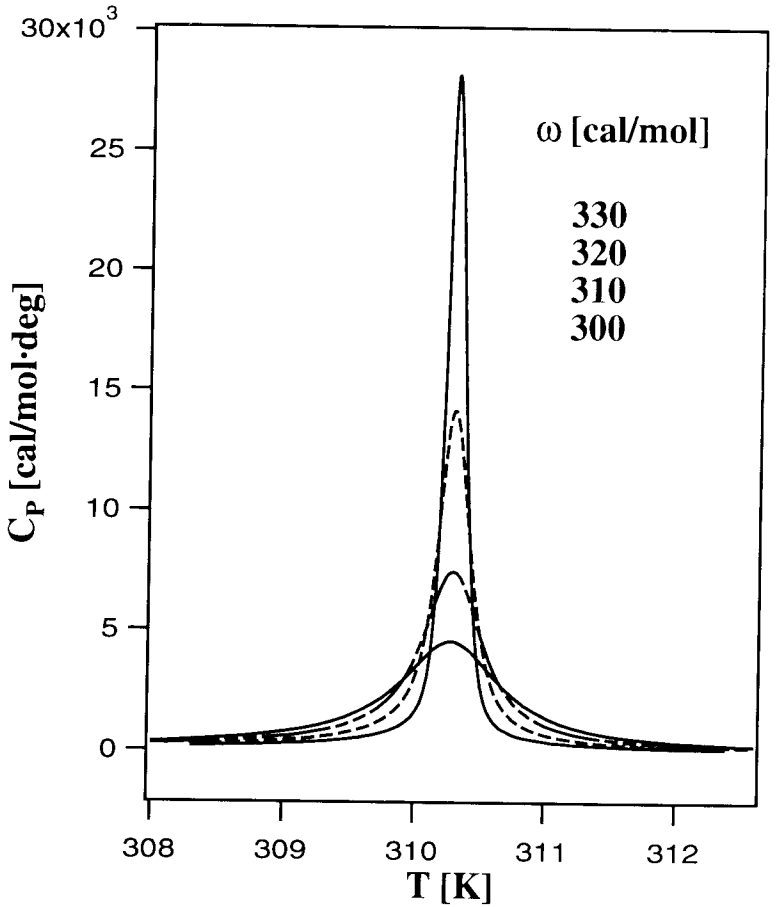


**Figure 9.** Heat capacity profiles for the chain-melting of a lipid bilayer with $\Delta H_t = 8.7$ kcal/mol, $T_m = 310.3$ K, calculated with a two-dimensional Ising model and unlike nearest-neighbor interaction free energies of $\omega_{gl} = 300, 310, 320, 330$ cal/mol, which are assumed to be purely enthalpic. Calculations were performed for a triangular lipid matrix with $31 \times 31$ sites by using a single Monte Carlo simulation (for $\omega_{gl} = 320$ cal/mol and $T = T_m$) and the Ferrenberg-Swendsen (1988) method with Equation 25.

the interfacial free energy parameter increases the cooperativity of the transition, resulting in both a decreasing transition half-width and an increasing heat capacity maximum.

Figure 10 shows representative lipid configurations obtained from Monte Carlo simulations for temperatures below, at, and above the heat capacity maximum of the chain-melting transition. As can be seen, the lipids form spatially separated domains of various sizes which are composed essentially of lipids in a single state (either gel or fluid). As the temperature changes towards the mid-point of the transition, the domains composed of lipids in the

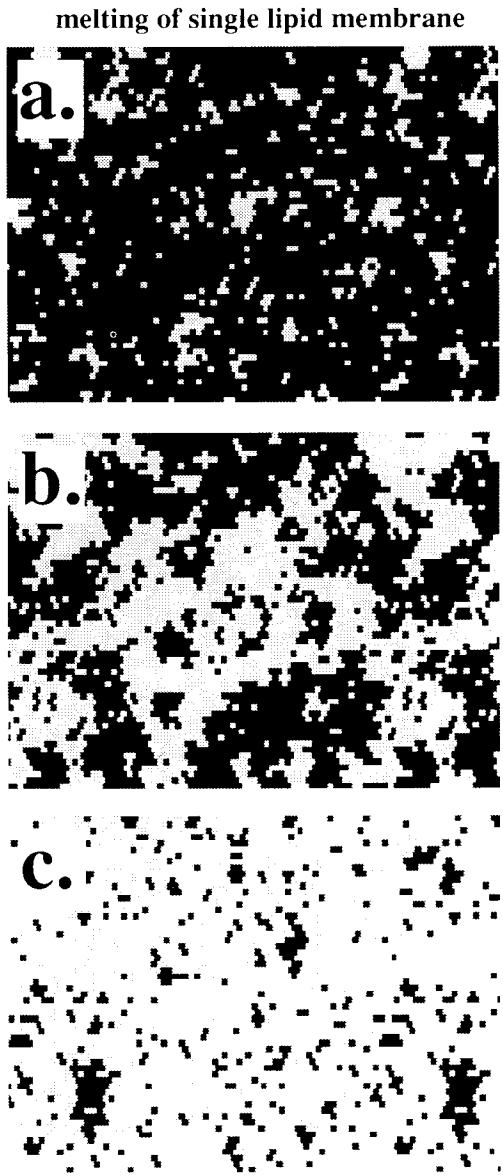


**Figure 10.** Snapshots of the lipid configuration at temperatures: (a) below ($T = 308.3$ K), (b) at ($T = 310.3$ K), and (c) above ($T = 312.3$ K) the heat capacity maximum for a lipid matrix with $61 \times 61$ sites, $\Delta H_t = 8.7$ kcal/mol, $\omega_{gl} = 310.3$ cal/mol and $\Delta S_t = 28$ cal/mol/K. For all these Monte Carlo simulations a triangular lattice with periodic boundary conditions was used. Gel-state lipids are black and fluid-state lipids are grey (Heimburg and Biltonen, 1996).

minority state grow in size at the expense of the majority state, achieving their maximum size at the transition mid-point. The tendency to domain formation results from the unfavorable interfacial energy between the gel and fluid lipid states and becomes increasingly more pronounced as the interfacial energy increases and the transition becomes more cooperative. On the other hand, as can be seen from Figure 10, the domain surface is complex and approximately fractal. This is a result of the energetically favorable increased entropy of a more extended interface. The unfavorable interfacial free energy (assumed here to be totally enthalpic) and the favorable entropy of an extended interface balance each other in a temperature-dependent manner. However, the higher the value of the enthalpic parameter $\omega_{gl}$, the larger the average domain size and the shorter the overall domain interface become. This is of importance in considering the distribution of bound proteins as described in the next section.

With increasing cooperativity one expects eventually to get into a regime where a continuous change in the lipid state, such as considered above, converts to first-order behavior. First-order transitions show a coexistence of two macroscopic states in the same canonical ensemble at the transition point which means that at the chain-melting point two membrane configurations with different fractions of fluid lipids are present with equal probability. This is demonstrated in Figure 11, in which the probability $P(f, \bar{n}_{gl})$ of finding a membrane with a fluid lipid fraction $f$ and a mean number of unlike contacts per lipid, $\bar{n}_{gl}$, at the transition point is plotted as a function of these two variables. The probabilities are obtained from the individual terms in the summation in Equation 25 with $X = 1$, $f = n_l/n$, and $\bar{n}_{gl} = n_{gl}/n$, where $n$ is the total number of lipids. As the cooperativity parameter increases, the distribution of states progressively develops two maxima (Figure 11d), which indicates first-order behavior (Lee and Kosterlitz, 1991). The fluctuations in such a highly cooperative system are shown in the lower panel of Figure 8. Rapid fluctuations take place about one of the maxima of Figure 11d, and then, less frequently, large-scale fluctuations take place between the two maxima. As the size of the system increases, the distributions in Figure 11d become sharper, and the large-amplitude fluctuations become more abrupt but less frequent. In the case of a low cooperativity (Figure 11a), only one maximum exists in the probability distribution. This corresponds to a second- or higher-order transition, because the system does not switch from one state to the other at the transition but undergoes a continuously varying change of state. The fluctuations in this type of low-cooperativity system correspond to those given in the upper panel of Figure 8.

Finally, it will be noted that the lateral compressibility of the lipid matrix also can be obtained from the Monte Carlo simulations for the two-state model. This is done in a manner similar to that described for the heat capacity (Hill, 1960), because the fluctuations in lipid surface area also are proportional to those in the fraction of fluid lipids. These elastic properties of the lipid membrane are considered in detail in a later part of the chapter.

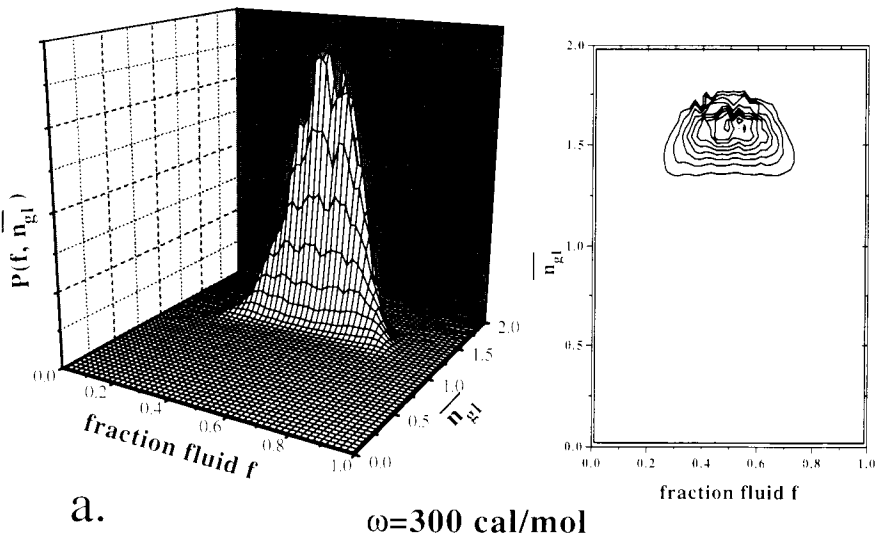


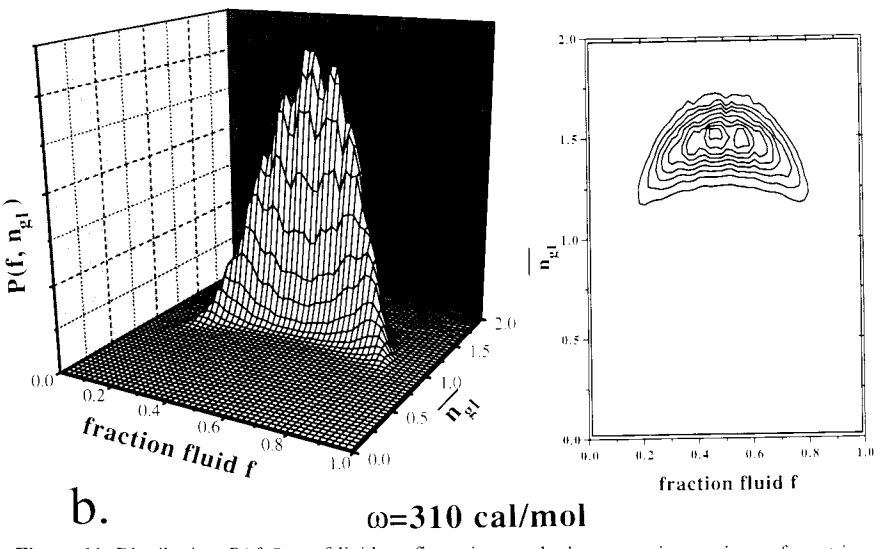


**Figure 11.** Distribution $P(f, \bar{n}_{gl})$ of lipid configurations at the heat capacity maximum for a triangular lipid matrix with 31 × 31 sites with increasing values (a to d) of the interaction energy, $\omega_{gl}$, between unlike lipids. Parameters used in the Monte Carlo simulations are those given in the legend to Figure 9. The probabilities $P(f, \bar{n}_{gl})$ are obtained from the individual terms in the summation of Equation 25, with $X = 1$, $f = n_l/n$ and $\bar{n}_{gl} = n_{gl}/n$, where $n$ (= 31 × 31) is the total number of lipids in the matrix. At higher values of $\omega_{gl}$ the distribution curve displays two maxima (panel d), indicative of a first-order transition, whereas a single maximum (panel a) is typical for second- or higher-order transitions.

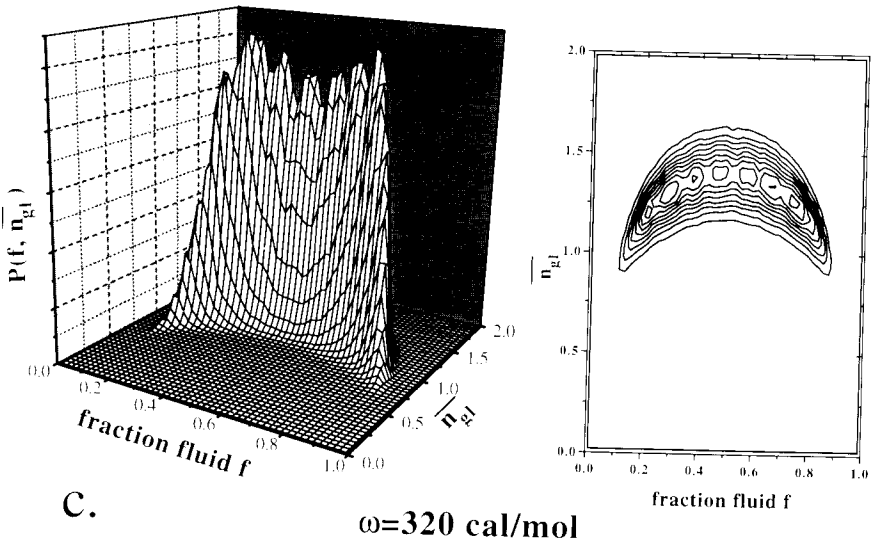


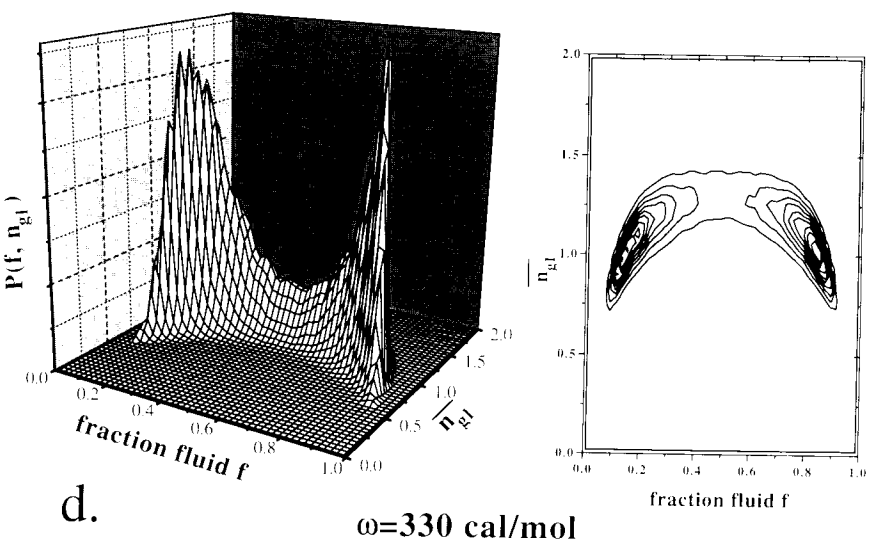


**Figure 11.** (Continued)

*Binding of Peripheral Proteins*

This section deals with the effects of binding peripheral proteins on the phase transition behavior of lipid bilayers and the coupling of protein binding and lipid phase state. The results can be analyzed using the two-state Ising model that was given for the lipid chain-melting transition in the previous section, together with the thermodynamics of protein binding discussed earlier. In addition, the Monte Carlo methods of the previous section may also be applied to investigate the protein distribution on the lipid surface.

CALORIMETRIC DATA

First we begin with some experimental results. In Figure 12, the heat capacity curves in the temperature range of the lipid chain-melting transition are given for bilayers of two different anionic lipids in the presence and absence of basic peripheral proteins. These thermograms have been measured by using differential scanning calorimetry. Concentrating on the left side of Figure 12 for dimyristoyl phosphatidylglycerol bilayers in the presence of cytochrome *c*, it can be seen that

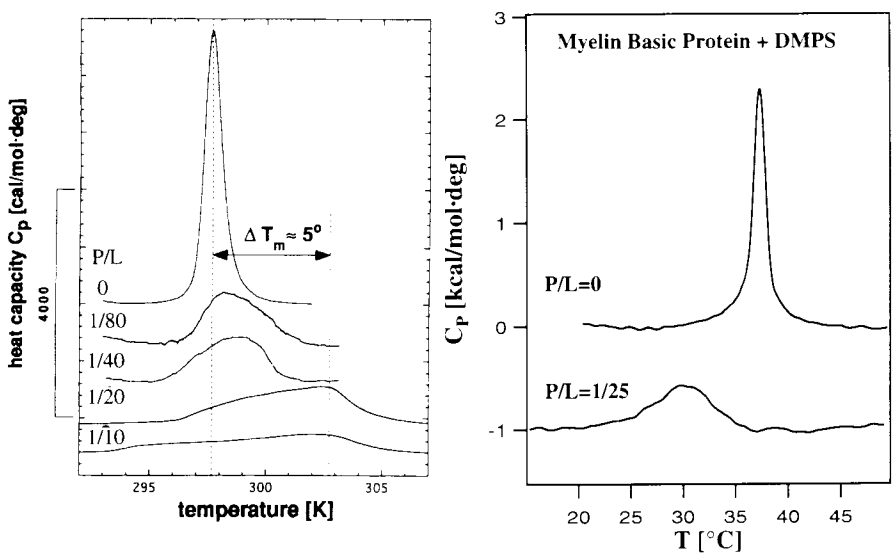


**Figure 12.** Heat capacity profiles obtained by differential scanning calorimetry for anionic lipid bilayers and lipid/protein complexes with peripheral proteins. Left: Dimyristoyl phosphatidylglycerol bilayers with cytochrome *c* bound at different degrees of surface saturation (from upper to lower: 0, 25, 50, 75, and 100%, assuming a lipid/protein stoichiometry of 10 mol/mol for saturation). The change in total integrated heat of transition upon saturation binding is −4.3 kcal/mol. (Adapted from Heimburg and Biltonen, 1996). Right: Dimyristoyl phosphatidylserine bilayers in the absence (upper) and in the presence (lower) of myelin basic protein (lipid/protein = 25 mol/mol). The change in total integrated heat of transition upon protein binding is −1.6 kcal/mol. (Adapted from Ramsay et al, 1986 with permission).

binding of increasing amounts of protein results in an asymmetric broadening of the transition and a shift in the heat capacity maximum to higher temperatures by approximately $\Delta T_m \approx +5°C$. These results are in qualitative agreement with the general considerations of the coupled protein binding and lipid phase equilibria given earlier (Figure 6). In addition, it has been found that the protein binding has a large effect on the transition enthalpy, which decreases from $\Delta H_t = 6.0$ kcal/mol for the lipid bilayers alone to $\Delta H_t = 1.7$ kcal/mol lipid in the presence of a saturating amount of protein bound. This represents a very significant energetic effect of protein binding.

The enthalpies of protein binding at saturation obtained in the cytochrome *c*/dimyristoyl phosphatidylglycerol system by titration calorimetry are given for different temperatures in Figure 13. It can be seen that the binding reaction is strongly endothermic, indicating that it must be entropy driven, at least in part by surface electrostatics. The binding enthalpy decreases strongly from $\Delta H_p = +6.8$ kcal/mol lipid in the gel phase to $\Delta H_p = +2.8$ kcal/mol lipid in the fluid phase, correlating with the large decrease in chain-melting enthalpy on

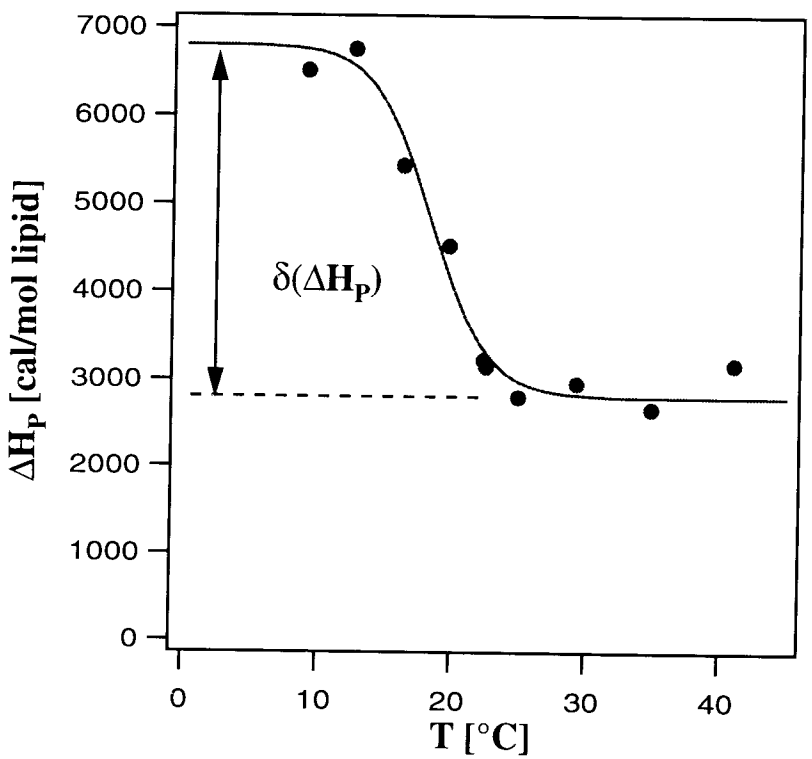


**Figure 13.** Total heat of binding a saturating amount of cytochrome *c* to dimyristoyl phosphatidylglycerol bilayers as a function of temperature, determined in a titration calorimeter. Note the strong change in enthalpy of the endothermic binding reaction in a region close to the lipid phase transition. (Adapted from Heimburg and Biltonen, 1994).

protein binding in Figure 12. This change is unrelated to the surface free energy of the electrostatic double layer, which in the high potential limit is entropic in origin and most probably arises from structural and hydrational changes in the lipid bilayer on protein binding. In addition, the temperature dependence of the enthalpy of protein binding (Figure 13) does not correspond in a one-to-one fashion with the degree of transition in the lipid state as deduced from Figure 12. This suggests a strong contribution from the heat capacity of binding to one or both of the lipid states (probably to the gel state because the large changes occur at lower temperature than the lipid transition mid-point and the binding enthalpy is essentially independent of temperature in the fluid state). The changes in heat of transition on protein binding and the changes in heat of binding on lipid transition may be related by the following thermodynamic scheme:

$$\begin{array}{ccc} L(9^{\circ}\mathrm{C}) + P & \xrightarrow{\Delta H_t^L} & L(41^{\circ}\mathrm{C}) + P \\ \Delta H_P^G \downarrow & & \downarrow \Delta H_P^F \\ LP(9^{\circ}\mathrm{C}) & \xrightarrow[\Delta H_t^{LP}]{} & LP(41^{\circ}\mathrm{C}) \end{array}$$

where $\Delta H_t^L$ and $\Delta H_t^{LP}$ are the lipid transition enthalpies for the lipid bilayers alone ($L$) and for the lipid-protein complex ($LP$), respectively, and $\Delta H_P^G$ and $\Delta H_P^F$ are the enthalpies of binding the protein ($P$) to gel-phase lipid (9°C) and to fluid-phase lipid (41°C). Because enthalpy is a thermodynamic state function, independent of pathway: $\Delta H_t^L + \Delta H_P^F = \Delta H_P^G + \Delta H_t^{LP}$, i.e., the decrease in protein binding enthalpy ($\Delta H_P^F - \Delta H_P^G = -4.0$ kcal/mol) should compensate that of the lipid transition ($\Delta H_t^{LP} - \Delta H_t^L = -4.3$ kcal/mol). This consistency suggests that the strongly endothermic enthalpy of protein binding is associated with structural and other changes in the lipid which are reflected in the strongly reduced chain-melting enthalpy (Heimburg and Biltonen, 1994).

Finally, we consider the shift in temperature of the lipid transition. For the lipid bilayers alone, the mid-point of the transition occurs at a temperature given by (Cevc and Marsh, 1987):

$$T_m^L = \frac{\Delta H_t}{\Delta S_t} \tag{30}$$

where $\Delta H_t = 6.0$ kcal/mol and $\Delta S_t = 20$ cal/mol/K for dimyristoyl phosphatidylglycerol. In the presence of a saturating amount of proteins, almost all lipids are in contact with a bound protein. It can be seen from the left-hand panel of Figure 12 that, for saturation binding of cytochrome $c$ to dimyristoyl phosphatidylglycerol, the heat capacity profile of the lipid transition is not symmetric. Nevertheless, the mid-point of the transition in the presence of a saturating amount of protein might be expected to occur at a temperature given approximately by:

$$T_m^{LP} = \frac{\Delta H_t + \delta \Delta H_p}{\Delta S_t + \delta \Delta S_p} \tag{31}$$

where $\delta\Delta H_p$ and $\delta\Delta S_p$ are the differences in enthalpy and entropy per lipid, respectively, for protein binding to the fluid and gel states (Heimburg and Biltonen, 1996). For cytochrome $c$ binding to dimyristoyl phosphatidylglycerol: $\Delta T_m \approx +5^\circ$ (Figure 12) and $\delta\Delta H_p \approx -4.3$ cal/mol (Figure 13), and, therefore, from Equation 31 one obtains a change in the entropy of protein binding on lipid chain-melting of $\delta\Delta S_p \approx -14.6$ cal/mol/K. The difference in free energy of protein binding to the fluid and gel lipid states, $\delta\Delta G_p = \delta\Delta H_p - T \cdot \delta\Delta S_p$, therefore exhibits a strong degree of entropy-enthalpy compensation. It has a net entropic value of $\delta\Delta G_p = +100$ cal/mol at 302 K (the approximate mid-point for the transition of the lipid-protein complex) and decreases to give complete compensation ($\delta\Delta G_p = 0$) at 295 K, i.e., 2 degrees below the transition of the lipid in the absence of protein. This sensitive temperature dependence of the free energy leads to a considerably asymmetric broadening of the lipid chain-melting transition (see Figure 12, left side). Indeed, experimentally observed transitions often are broadened to such an extent that it is difficult to resolve the transition maximum, suggesting that the binding of proteins involves considerable entropic contributions.

Applying the same principles of analysis to the data for the binding of myelin basic protein to dimyristoyl phosphatidylserine that are given in the right-hand panel of Figure 12, it can be inferred that the difference in enthalpy of protein binding is $\delta\Delta H_p \approx -1.6$ kcal/mol lipid, and, from the transition shift, that the difference in entropy of binding is $\delta\Delta S_p \approx -4.8$ cal/mol/K. Here also, there is a considerable degree of entropy-enthalpy compensation but the difference in net free energy of protein binding is enthalpic, $\delta\Delta G_p \approx -135$ cal/mol lipid, at the transition temperature of the lipid-protein complex. In this case, the free energy difference is negative, corresponding to the downward shift in temperature of the transition on protein binding.

These two experimental examples demonstrate that considerable insight can be gained into the nature of the lipid-protein interaction by a detailed study of the thermodynamic behavior. It is clear that there can be very sizeable enthalpic contributions to the binding free energy that do not arise from changes in the electrostatic double layer free energy, which in the high potential limit is almost totally entropic. Also, there must be considerable entropic contributions that do not have their origin in the electrostatic double layer because the difference in entropy of binding is found to be much greater than that predicted by the entropic contribution in Equation 20 from double-layer theory. It is noted that these differences are unlikely to arise from the short-comings of Gouy-Chapman electrostatic double-layer theory because, if anything, this theory tends to overestimate the energetics of lipid-chain melting (Cevc et al, 1981; 1980).

Generally, the nonelectrostatic contributions to the binding energy express themselves in the intrinsic binding constant, $K$, that was considered earlier. Possible sources for these contributions are structural and conformational changes in both protein and lipid, changes in hydration and hydrogen bonding, and possibly even hydrophobic interactions. Tertiary structural and conformational changes in cytochrome $c$ have been found on binding to anionic lipids, and there

can be morphological changes in the bilayer as well (Heimburg and Marsh, 1993; Heimburg et al, 1991; Muga et al, 1991). Considerable changes occur in the secondary structure of myelin basic protein on binding to negatively charged lipids (Surewicz et al, 1987). Evidence for dehydration of the lipid surface on binding peripheral proteins has come from other spectral studies (Jain and Vaz, 1987; Sankaram et al, 1990). Binding of cytochrome *c* (Görrisen et al, 1986), myelin basic protein (Sankaram et al, 1989a), as well as other proteins (Sankaram et al, 1989b), has a marked effect on lipid mobility and hence potentially on the energetics of chain packing and possibly also of the chain configuration. Additionally, there is evidence for penetration of myelin basic protein into the hydrophobic region of the lipid bilayer (Boggs et al, 1988; London et al, 1973; Sankaram et al, 1989a). Thermodynamic studies, as described above, can give some indication of the relative energetic significance of these different structural and hydrational changes. However, considerable entropy-enthalpy compensation may also take place in the individual binding reactions, as is found for the differences in binding to the gel and fluid states.

## SIMULATIONS

Now we return to the two-state Ising model by considering the effects of protein binding on the lipid state. A strictly local model is taken for the lipid-protein interaction (see Figure 14, upper); the peripheral proteins are assumed to affect only those lipids situated directly under them. (For ionic strengths of 10 mM and above, at which the Debye length of the electrolyte is of the order or less than a typical protein diameter, such an assumption is not strongly at variance with the nonlocalized double-layer approach used for the surface electrostatic interactions earlier.) For a lipid in contact with a peripheral protein, the statistical weight $K(T)$ that determines the probability to switch from the gel to the fluid state in a Monte Carlo step becomes:

$$K(T) = \exp\left(-\frac{\Delta H_t - T\Delta S_t + \Delta n_{gl} \cdot \omega_{gl} + \Delta E_P}{RT}\right) \tag{32}$$

whereas it is given by Equation 27 in the absence of proteins. Here, the differential free energy of protein binding, $\delta\Delta G_P$, is approximated by a simple enthalpic term, $\Delta E_P$. In addition to the switching of the lipid states, the proteins are also allowed to rearrange laterally on the lipid surface. Translational steps for a protein are favored in a direction for which the strength of binding increases. This, in turn, depends on the distribution of gel and fluid lipids. For a given lipid arrangement the probability for translation in one of the six possible directions on a triangular lattice is given by:

$$P_m(i) = \frac{K_m(i)}{1 + K_m(i)} \tag{33}$$

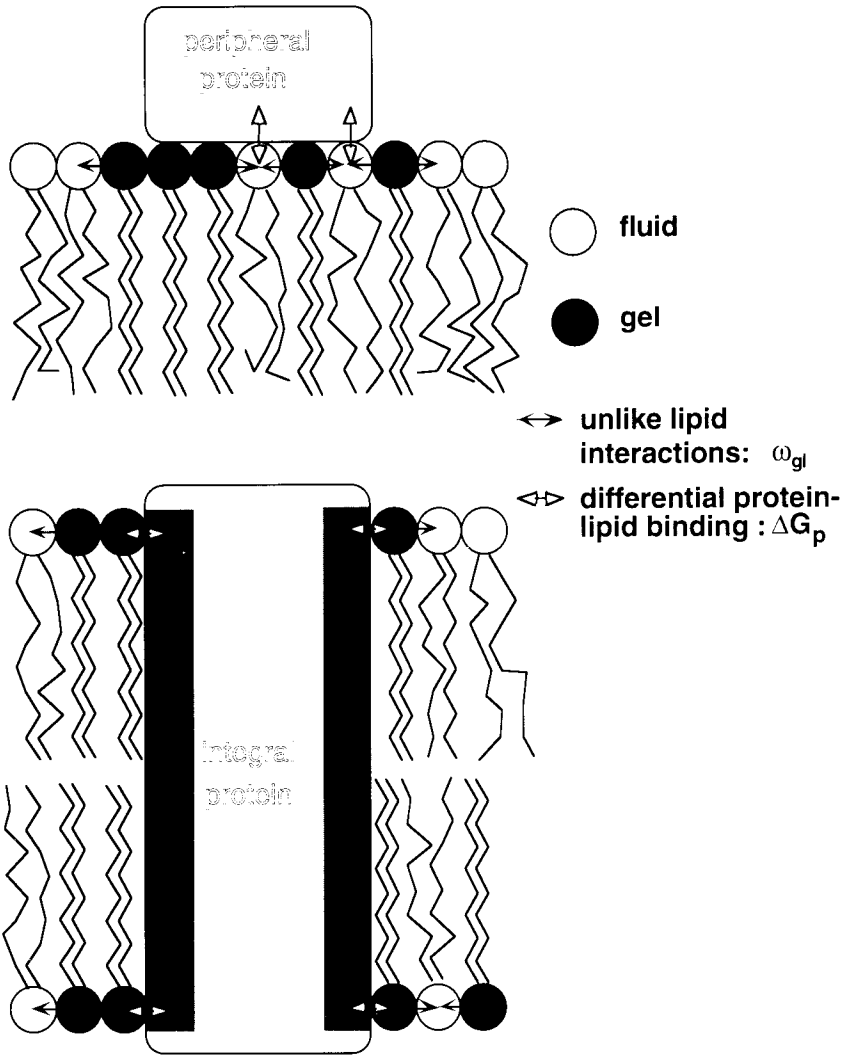


**Figure 14.** Schematic illustration of the local interactions between proteins and lipids, and the coupling with the interactions between unlike lipids. Upper: peripheral protein; lower: integral protein. Energetically less favorable interactions, characterized by the excess free energies $\omega_{gl}$ and $\delta\Delta G_P$, are indicated by arrows (Heimburg and Biltonen, 1996).

where the index $i$ represents the six different directions. The statistical weights are given by:

$$K_m(i) = \exp\left(-\frac{\Delta n_l(i) \cdot \Delta E_P}{RT}\right) \tag{34}$$

where $\Delta n_l(i)$ is the increase in the number of fluid lipids with which the protein is associated. Using a random number generator the proteins are moved from

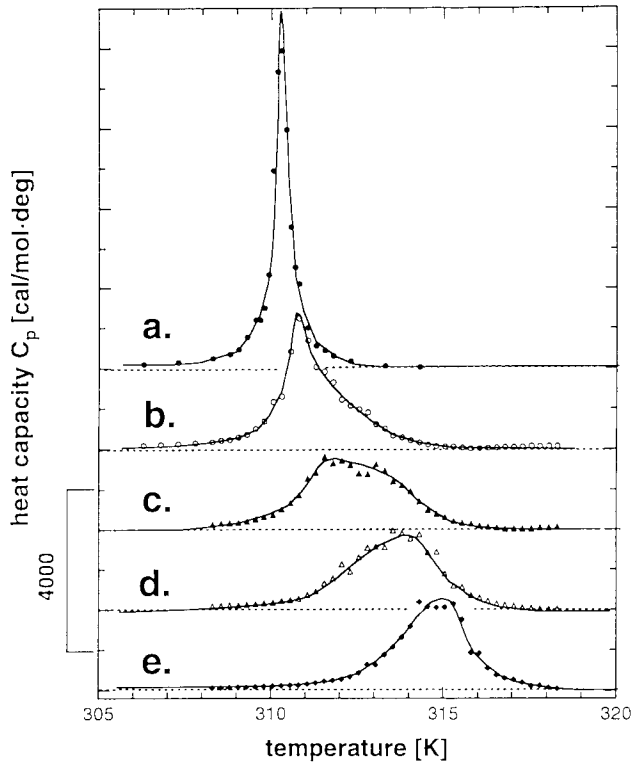


**Figure 15.** Heat capacity profiles calculated from Monte Carlo simulations for the two-state chain-melting of a lipid membrane with varying amounts of peripheral protein bound. Calculations were performed for a lipid matrix of $61 \times 61$ sites with $\Delta H_l = 8.7$ kcal/mol, $T_m = 310.3$ K, $\omega_{gl} = 310.3$ cal/mol. Each protein covers 19 lipid sites and has a differential binding energy with the two lipid states of $\Delta E_P = 200$ cal/mol. The five different profiles correspond to degrees of surface saturation (from upper to lower) of 0, 16, 32, 48, and 64%, or protein/lipid ratios of 0, 1/125, 1/62, 1/41, and 1/31 mol/mol, respectively. (Adapted from Heimburg and Biltonen, 1996).

an initial statistical distribution in one of the six possible directions with the probability $P_m(i)$ (Heimburg and Biltonen, 1996).

Simulations are performed by alternating readjustment of single lipid states and recalculation of the protein positions. Figure 15 shows the heat capacity profiles calculated from Monte Carlo simulations for a peripheral protein with a cross section equal to that of 19 lipid molecules (approximately equivalent to phospholipase $A_2$) and a differential gel-fluid protein binding energy of $\Delta E_P = +200$ cal/mol (enthalpic). The parameters for the lipid matrix are: $\Delta H_l = 8.7$ kcal/mol, $T_m = 310.3$ K and $\omega_{gl} = 310.3$ cal/mol, which are similar to those found for dipalmitoyl phosphatidylcholine small unilamellar vesicles (Mouritsen and Biltonen, 1992; Sugar et al, 1994). It can be seen that the heat capacity maxima are shifted progressively to higher temperatures, and the profiles are broadened asymmetrically as increasing numbers of proteins are

bound. Although the simulation parameters are rather different from those found for the binding of cytochrome *c* to dimyristoyl phosphatidylglycerol, there is a remarkable qualitative similarity between the calculated heat capacity profiles in Figure 15 and the experimental data in Figure 12 (left panel). The differential binding energy was chosen in the simulations to give a shift of the transition mid-point at saturation binding of $+7^{\circ}$ and therefore produces a shift in the transition comparable to that in Figure 12, at less than saturation binding. To produce a downward shift in the transition on protein binding, such as that observed in the right-hand panel of Figure 12, would require $\Delta E_P$ to have a negative sign. Inclusion of entropic contributions to the differential free energy of binding, such as is suggested by the experimental data, would produce a more pronounced asymmetric broadening of the heat capacity profiles.

The distribution of the proteins on the lipid surface is shown in Figure 16, which gives representative configurations of the protein and lipid at temperatures below, within, and above the chain-melting transition. It can be seen that the proteins preferentially accumulate and cluster on the lipid gel domains that are present in the transition region. This is because the free energy of binding to the gel domains is lower than that to the fluid domains, for a positive value of $\Delta E_P$. Correspondingly, gel domains form preferentially at the locations of the protein molecules. The degree of protein clustering can be characterized by the deviation of the mean separation between adjacent proteins obtained in a simulation from that expected for a random distribution:

$$C(T) = \frac{d_{\text{random}} - d(T)}{d_{\text{random}} - d_{\text{minimum}}} \tag{35}$$

where $d_{\text{random}}$, $d_{\text{minimum}}$ and $d(T)$ are the mean distances between neighboring proteins for a random distribution, for closest packing, and from the simulation results at temperature $T$, respectively. As shown in Figure 17, the protein cluster parameters $C(T)$, derived from distributions such as those in Figure 16, show a distinct maximum at temperatures close to, or on the gel-phase side of, those of the heat capacity maxima. This aggregation is a necessary accompaniment to the shift in the heat capacity curve.

*Integral Proteins*

In this section, we briefly consider lipid interactions with integral membrane proteins. The intention is not to give a comprehensive discussion (Marsh, 1995a, 1985) but rather to concentrate on the different interaction of the integral protein with lipids in the different phases, within the context of the two-state model (see Figure 14, lower panel). In general, it is to be expected that integral proteins will interact and mix differently with lipids in the fluid and gel states. There is considerable evidence from freeze-fracture electron microscopy that integral proteins frequently tend to aggregate in gel-phase lipid membranes, whereas they are more randomly distributed within the fluid lipid phase. Clear examples are, for instance, the $Ca^{2+}$-ATPase (Kleeman and McConnell, 1976),

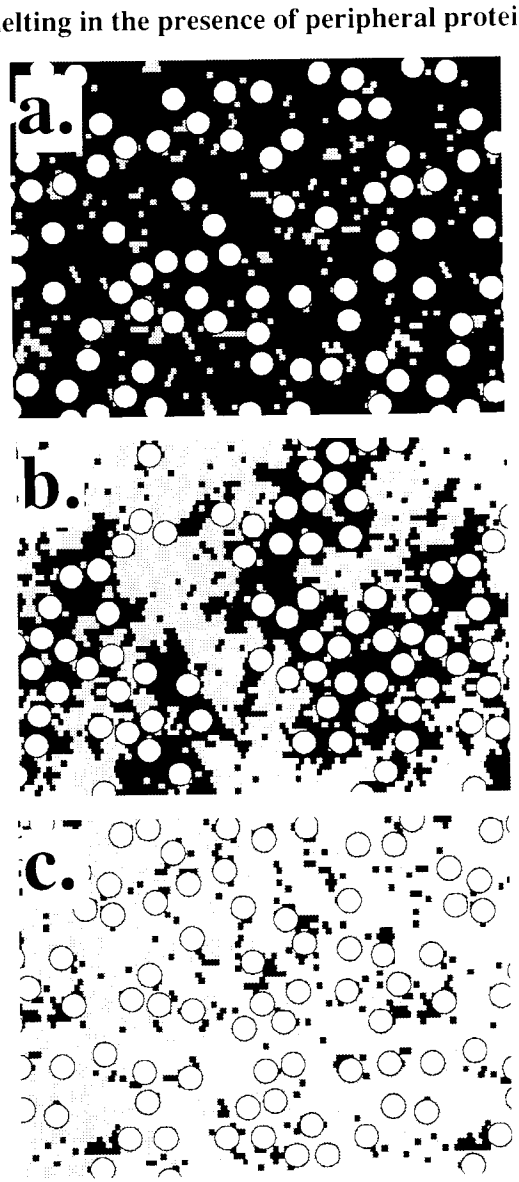


**Figure 16.** Snapshots of the configuration of a $61 \times 61$ lipid matrix with 60 surface-bound peripheral proteins (each covering 19 lipid cross sections) at temperatures (a) below ($T = 306.3$ K), (b) at ($T = 312.3$ K), and (c) above ($T = 318.3$ K) the heat capacity maximum. Monte Carlo simulations were performed as for Figure 15 with $\Delta H_t = 8.7$ kcal/mol, $\omega_{gl} = 310.3$ cal/mol, $T_m = 310.3$ K, and $\Delta E_P = 200$ cal/mol. Gel-state lipids are black, fluid-state lipids are grey, and proteins are represented by white circles (Heimburg and Biltonen, 1996).

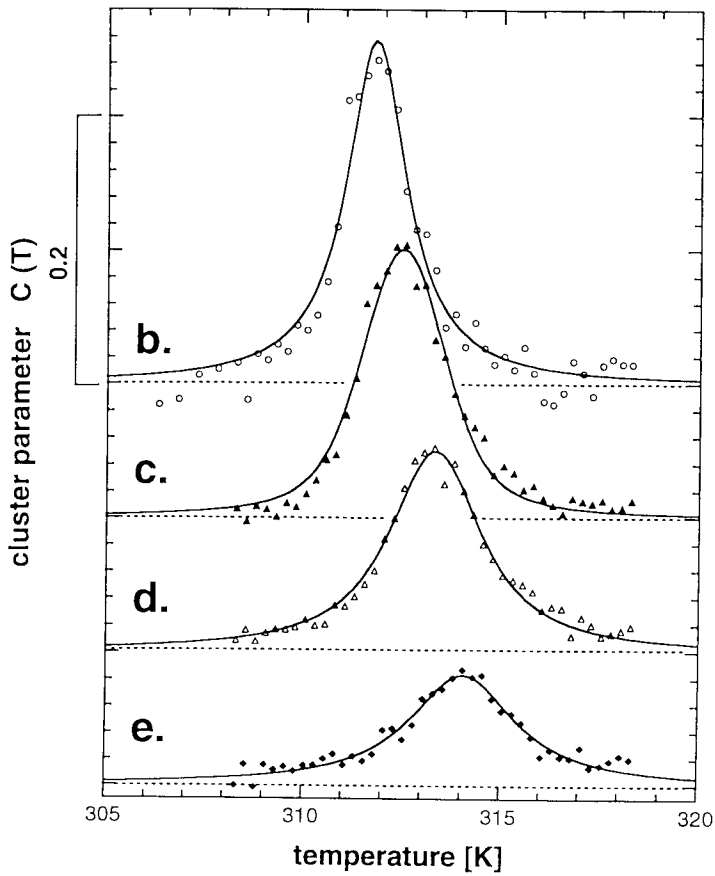


**Figure 17.** Aggregation profiles for peripheral proteins, corresponding to the calculated heat capacity profiles of Figure 15. The protein cluster parameters calculated from Monte Carlo simulations (Figure 16) are for protein/lipid ratios of (from upper to lower): 1/125, 1/62, 1/41, and 1/31 mol/mol. (Adapted from Heimburg and Biltonen, 1996).

cytochrome oxidase (Fajer et al, 1989), myelin proteolipid protein (Boggs et al, 1980), and glycophorin (Grant and McConnell, 1974), as well as membranes from fatty acid-supplemented *Escherichia coli* auxotrophs (Kleeman and McConnell, 1974). Matching of the hydrophobic span of the integral protein with that of the lipid chains in the different states is likely to play an important role (Marsh, 1995a,b). Hydrophobic matching may also play a role in the mixing properties with lipids of different chainlength in a single lipid phase, as is found for rhodopsin (Chen and Hubbell, 1973; Ryba and Marsh, 1992). In addition, any preferential interaction between proteins, relative to the lipid-protein interactions, will tend to induce protein aggregation, which may again be dependent on the lipid state. An example of this is the well-known propensity of the band

3 anion transport protein to aggregate in fluid-phase lipids (Mühlebach and Cherry, 1985).

If, in the model of the previous section, the differential interaction energy, $\Delta E_P$ between the peripheral protein and the gel and fluid states of the lipid membrane is allowed to become extremely large, all lipids beneath the protein remain in the gel state, even at high temperatures. Conversely, with a very strongly negative value for the differential binding energy, domains consisting entirely of fluid lipid form beneath the peripheral protein. This can be used to mimic the thermodynamic behavior of integral proteins, if it is assumed that these all-gel or all-fluid domains beneath the protein represent the membrane-spanning core of the protein. In determining the thermodynamic observables (heat capacity, compressibility, etc.) the lipids in these cores must be excluded because they are considered to be part of the integral protein. This integral core interacts with the surrounding lipid in the same manner as do gel-phase lipids (in the case of a strongly positive value of $\Delta E_P$), or as do fluid-phase lipids (in the case of a strongly negative $\Delta E_P$). Clearly this is a considerable oversimplification of the actual situation because it assumes that the interaction of integral proteins with the two lipid states is identical with that of lipids in the complementary state, i.e., gel with fluid or fluid with gel, as described by the excess free energy $\omega_{gl}$. Nevertheless, the model contains all the qualitative features of a different protein interaction with the two lipid states (Heimburg and Biltonen, 1996). In the case of peripheral proteins with moderate values of the differential interaction energy $\Delta E_P$, the aggregation of such proteins at the phase transition (see Figure 16) is caused by different interactions with the lipid domains, which are created primarily by the different lipid chain interactions. This type of interaction disappears outside the transition range, and the distribution of such proteins then becomes random, in the absence of specific protein-protein interactions. In contrast to this, the lipid interface with integral proteins (or with the lipids beneath a peripheral protein to which they bind extremely strongly) exists at all temperatures. As will be seen in the following, this affects the aggregation profile of the protein, which in turn shows up in the heat capacity profiles for lipid chain-melting.

We consider here the simulated heat capacity profiles for a hypothetical integral protein corresponding to a highly positive value of $\Delta E_P$, i.e., with a preference for the gel phase. The cross section of the protein is assumed to correspond to 19 lipid cross sections and, for a compact structure, will have a comparable number of nearest-neighbor true lipids in its boundary shell. The calculation is performed by using the same approach as that used for peripheral proteins, as outlined in the previous section. The integral cores of the hypothetical protein consist of gel-phase lipids that do not undergo a change of state and are not counted in calculating the heat capacity. As can be seen from Figure 18, the heat capacity profiles calculated from the Monte Carlo simulations for this model shift to higher temperatures with increasing effective protein/lipid ratio. This aspect of the behavior is similar to that for peripheral proteins with smaller positive values of $\Delta E_P$ (see Figure 15). However, the shape of the heat capac-

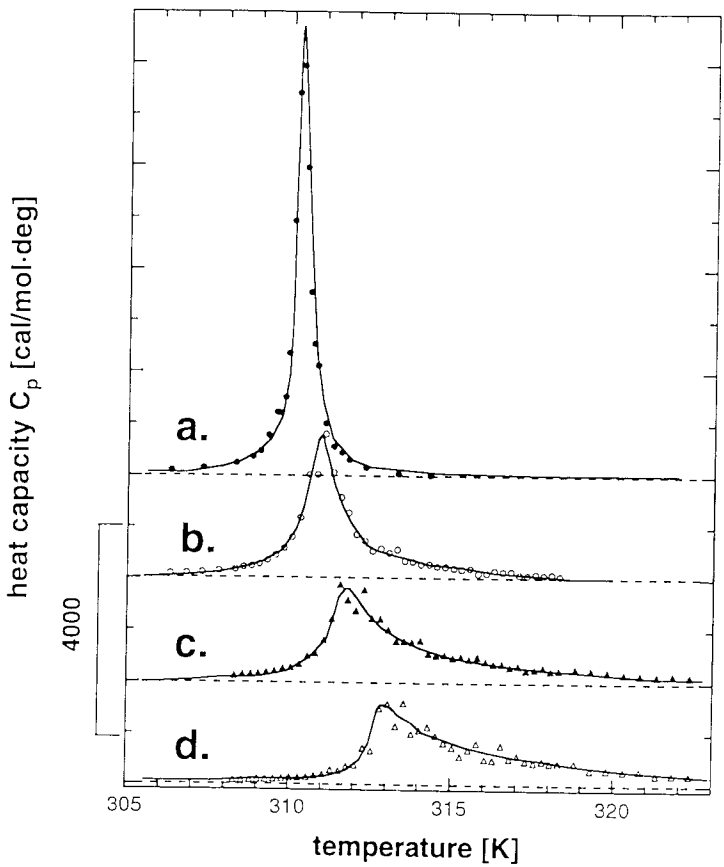


**Figure 18.** Heat capacity profiles calculated for a lipid matrix containing different amounts of a hypothetical integral protein that is modeled as a cluster of 19 permanently gel-state lipids. Monte Carlo calculations were performed for a lipid matrix of 61 × 61 sites with $\Delta H_t = 8.7$ kcal/mol, $T_m = 310.3$ K, and $\omega_{gl} = 310.3$ cal/mol (equal also to the excess interaction energy of the protein with a fluid-state lipid). The four different profiles correspond to protein/lipid ratios of (from upper to lower) 0, 1/105, 1/43, and 1/22 mol/mol. (Adapted from Heimburg and Biltonen, 1996).

ity profiles is different from the latter case. In the case of Figure 15, the heat capacity profiles display a maximum at the lower end of the transition for low degrees of surface coverage by the protein, whereas the maximum shifts to the upper end of the transition profile for high degrees of protein occupancy. This change arises from the change in number of lipids in contact with the protein for increasing numbers of proteins bound. The heat capacity profiles in Figure 18, however, always display a maximum at the low temperature end of the transition (in the case of a highly positive value of $\Delta E_P$). In the case of a preference of the protein for the fluid-phase lipids (highly negative values of $\Delta E_P$), the heat capacity profiles would shift downwards and display the heat capacity maximum at the upper end of the transition profile.

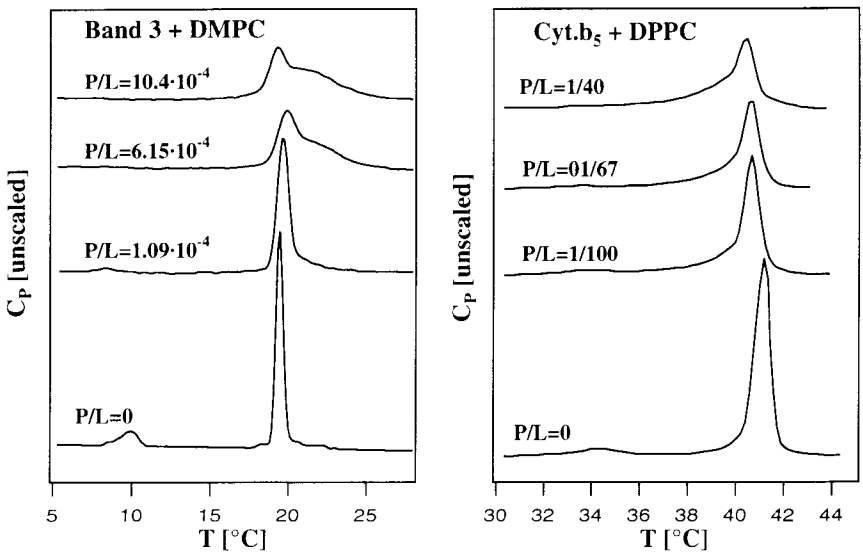


**Figure 19.** Experimental heat capacity profiles of lipid complexes with integral proteins. Left: Band 3 anion transport protein from erythrocytes reconstituted with dimyristoyl phosphatidylcholine at protein/lipid ratios of (from lower to upper): 0, 1/9200, 1/1630, and 1/960 mol/mol. (Adapted from Morrow et al, 1986). Right: Cytochrome $b_5$ reconstituted with dipalmitoyl phosphatidylcholine at protein/lipid ratios of (from lower to upper): 0, 1/100, 1/67, and 1/40 mol/mol. (Adapted from Freire et al, 1983 with permission).

The results of the model calculations that are given in Figure 18 can be compared with experimental heat capacity profiles for the chain-melting of lipid membranes reconstituted with purified integral membrane proteins. The left panel of Figure 19 shows heat capacity profiles for bilayers of dimyristoyl phosphatidylcholine that contain varying amounts of the band 3 protein of erythrocytes. These display a peak at a temperature close to that for the lipid alone and a high-temperature shoulder, which becomes progressively more pronounced as the protein concentration in the membrane increases. The right panel of Figure 19 gives heat capacity profiles for bilayers of dipalmitoyl phosphatidylcholine containing increasing amounts of cytochrome $b_5$ which display a similar but inverse behavior to that in the left panel. The heat capacity maximum here again does not shift with increasing protein content, but a shoulder develops now to the low-temperature side of the transition curve. These results resemble qualitatively the behavior of the model calculations in Figure 18 (and corresponding ones for highly negative $\Delta E_P$). As can be seen in the experimental examples, however, the shift of the heat capacity maximum can be small. Whereas the upward shift in heat capacity maximum in Figure 18 is consistent with the preferential affinity of the hypothetical integral protein for the gel-phase lipid, the near constancy of the lower boundary of the experimental heat capacity curves in the left panel of Figure 19 could be consistent with immiscibility of the band

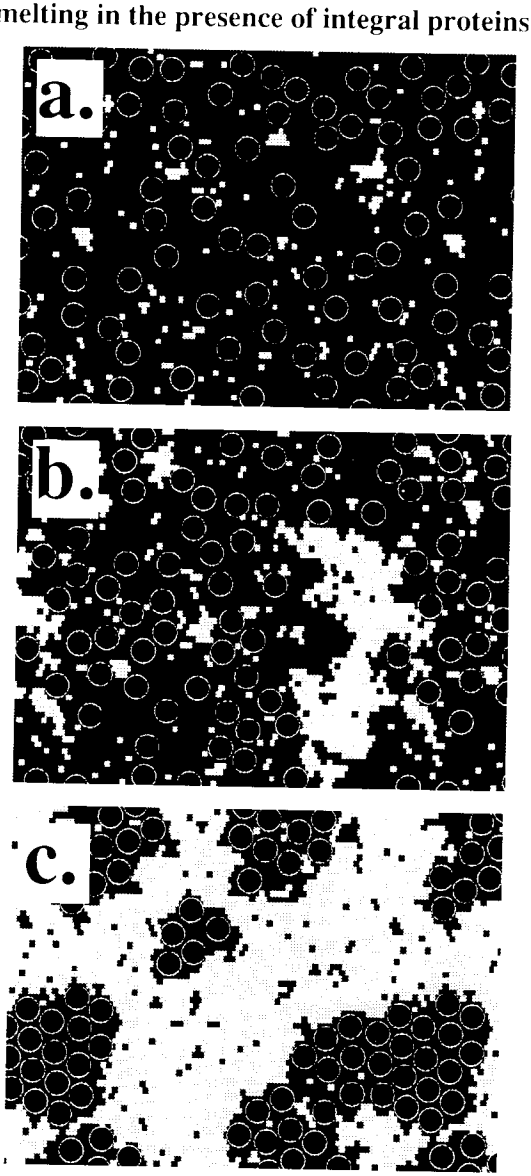


**Figure 20.** Snapshots of the configuration of a 61 × 61 lipid matrix containing 60 hypothetical integral proteins (modeled as a cluster of 19 gel-state lipids) at temperatures (a) below ($T$ = 306.3 K), (b) at ($T$ = 311.3 K), and (c) above ($T$ = 318.3 K) the heat capacity maximum. Monte Carlo simulations were performed as for Figure 18 with $\Delta H_l$ = 8.7 kcal/mol, $T_m$ = 310.3 K, and $\omega_{gl}$ = 310.3 cal/mol (equal also to the protein excess interaction energy with a fluid-state lipid). Gel-state lipids are black (stippled), fluid-state lipids are grey, and integral proteins are represented by black circles (Heimburg and Biltonen, 1996).

3 protein in the gel phase. Clearly, effects such as the latter would require the additional specification of lipid-protein and protein-protein interaction energies that are distinct from those which are represented in the current model solely in terms of lipid-lipid interactions.

In Figure 20, representative views of the lipid configuration and the protein distribution obtained from the model of Figure 18 are given for temperatures below, within, and above the chain-melting transition region. The protein has a near-random distribution at lower temperatures for which the lipid is predominantly in the gel state. As the temperature is increased, the proteins then cluster progressively in the domains of gel-state lipid that remain above the chain-melting point. This is reflected in the temperature dependence of the protein cluster parameter (Equation 35) that is given in Figure 21 for results calcu-

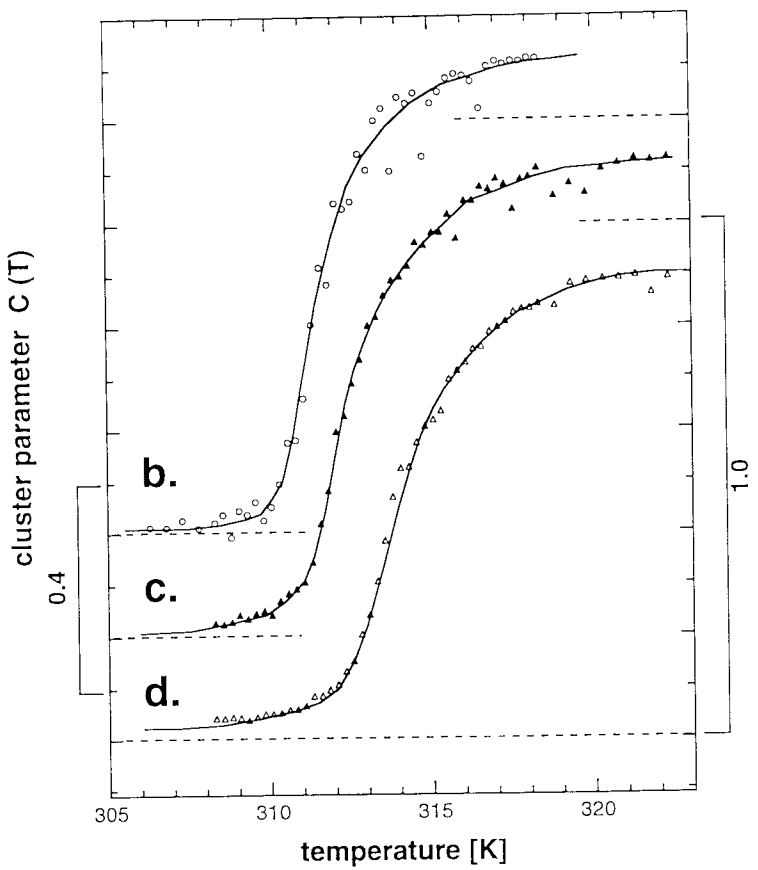


**Figure 21.** Calculated aggregation profiles for hypothetical integral proteins modeled as a cluster of 19 permanently gel-state lipids, using the simulation parameters from Figure 18. The protein cluster parameters are calculated from Monte Carlo simulations (Figure 20) with effective protein/lipid ratios of (from upper to lower): 1/105, 1/43, and 1/21 mol/mol. (Adapted from Heimburg and Biltonen, 1996).

lated with the model of Figure 18 at different protein contents. As can be seen, the proteins rapidly become progressively more aggregated (or clustered) as the temperature increases and the bulk of the lipid converts to the fluid state. The clustering profiles are shifted to higher temperatures as the protein concentration is increased. This can be rationalized as follows: when the chains of lipids in the presence of proteins that prefer gel-state lipids progressively melt as the temperature is increased, the proteins become more and more restricted to the few remaining gel domains. Simultaneously, protein-protein contacts become more favorable in order to avoid contacts of the protein with fluid lipids. This is a consequence of the hydrophobic core of the integral proteins being modeled as gel-state lipids and having a permanent interface with the free lipids. Quite generally, irrespective of model or mechanism, one will expect the aggregation profiles for integral proteins to reflect the preference for partitioning between the different lipid phases, and this will show up in the behavior of the heat capacity profiles.

Within the context of the model proposed in this section, the lipid interactions with integral membrane proteins are represented as an extreme case of the interactions with peripheral proteins. Nevertheless, comparison of Figure 18 with Figure 15, together with the energetic considerations discussed earlier, does indicate that there can be qualitative differences in the heat capacity profiles for lipid chain-melting between membranes containing integral proteins and those with surface-bound peripheral proteins that interact purely by their effects on the electrostatic double layer. As already discussed (Figures 17 and 21), this reflects a very different profile of protein clustering for peripheral proteins that do not interact extremely strongly with the lipid surface. In the case of complex lipid mixtures, of interactions with peripheral proteins that have a strong degree of enthalpy-entropy compensation, or particularly of peripheral proteins that bind extremely strongly, these distinctions might not be quite so clear.

## Discussion

A major goal of this chapter has been to demonstrate the thermodynamic linkage between protein binding, lipid mixing, lipid chain-melting, and domain formation, as well as protein aggregation, in membranes. In this final main section, we first review some of the consequences that lipid chain-melting and different interactions of proteins with the different lipid states may have on the function of membrane-associated proteins. This is done by taking examples of membrane proteins reconstituted with defined phospholipids. We then go on to consider the elastic properties of membranes, particularly in situations in which there is a coexistence of gel and fluid lipid states and the lateral membrane compressibility differs radically from that for membranes in a single lipid state. The lateral membrane compressibility most likely controls the readiness with which conformational changes may take place in integral proteins, those for which a conformational change is accompanied by a change in cross-sectional area.

Additionally, compressional waves within the membrane constitute a possible channel of communication between both surface-bound and integrally incorporated proteins.

### *Coupling of Protein Function to Lipid State*

The study of proteins in association with membranes of a single lipid species provides insight into the nature of the thermodynamic interactions that may control protein function. Examples are given here of various studies with such well-defined systems that contain a single type of peripheral or integral protein. The highly cooperative nature of the lipid chain-melting transition, and the clearly characterized structural and thermodynamic changes that accompany it, afford an unambiguous illustration of the dependence of protein function on the state of the lipid.

## FUNCTIONAL ASPECTS: PERIPHERAL PROTEINS

As examples of the conformational response of peripheral proteins to the state of lipid membranes, mitochondrial cytochrome *c*, and pancreatic or snake venom phospholipase $A_2$ will be discussed.

Cytochrome *c* is a peripheral membrane protein that functions as an electron carrier in the mitochondrial respiratory chain. This protein is associated at the outer face of the inner membrane, which contains a relatively high concentration of charged lipids, most notably of the unique mitochondrial lipid cardiolipin (Daum, 1985). The affinity of cytochrome *c* for electrons is determined by its redox potential. It has been found that the protein can assume at least two different conformational states, which have very different redox potentials (Hildebrandt and Stockburger, 1989a,b). The equilibrium between these two states is influenced by the potential applied to metal electrodes to which the protein is absorbed. Furthermore it has been found that a similar change in conformational state can be induced by the binding of cytochrome *c* to charged lipid membranes (Hildebrandt et al, 1990). Figure 22a shows the temperature dependence of the ratio of the two conformational states of cytochrome *c* bound to membranes of dimyristoyl phosphatidylglycerol, as recorded by the resonance Raman spectra of the haem group. As can be seen from the figure, the relative population of the conformational state II, which is characterized by a more negative redox potential, increases considerably in the temperature interval around 25°C, as a result of the chain-melting in the lipid/protein complex (Figure 12, left). Cytochrome *c* bound to dioleoyl phosphatidylglycerol, which is entirely in the fluid state throughout this range, displays no temperature dependence of this conformational equilibrium (Heimburg et al, 1991). In addition, it has been found that the states of cytochrome *c* bound to dimyristoyl phosphatidylglycerol above and below the chain-melting transition differ in their tertiary structure because they are characterized by significantly different hydrogen exchange kinetics of the amide backbone (Heimburg and Marsh, 1993). In Figure 22b, the

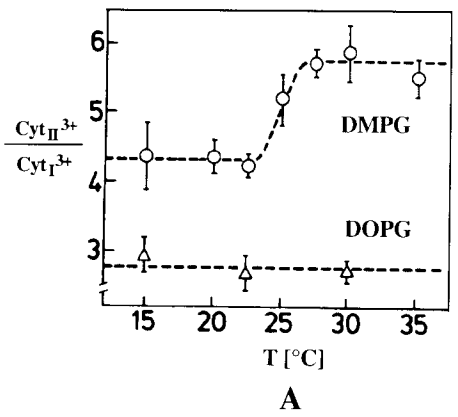


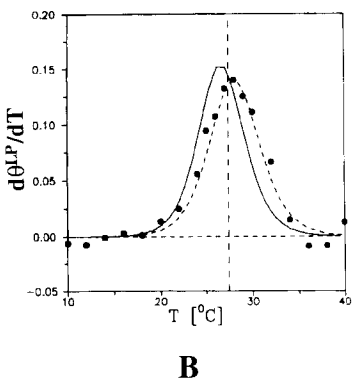


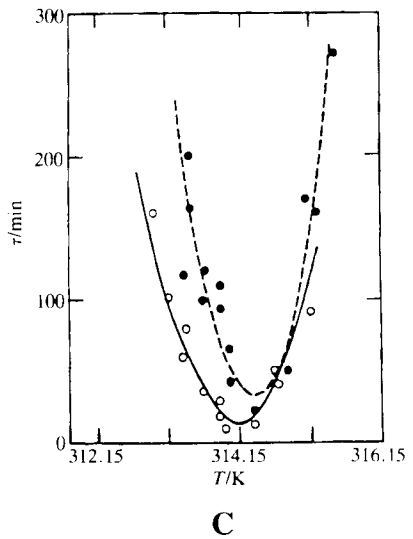


**Figure 22.** (a) Temperature dependence of the conformational equilibrium of the states cyt $c_{II}$ and cyt $c_I$ of cytochrome *c* bound to bilayers of dimyristoyl (○) and dioleoyl (△) phosphatidylglycerol, as determined by resonance Raman spectroscopy. (Adapted from Heimburg et al, 1991). (b) Temperature dependence of derivative curves for the degree of transition $\theta^{L,P}$ between the tertiary structural states of cytochrome *c* bound to dimyristoyl phosphatidylglycerol that have different amide proton exchange kinetics (solid line), and for the chain-melting transition of the lipid (dashed line). Exchange kinetics were measured by monitoring the protein amide I band and chain-melting by monitoring the lipid carbonyl band in the Fourier-transform infrared spectrum. (Adapted from Heimburg and Marsh, 1993). (c) Temperature dependence of the lag time, τ, for achieving the maximum hydrolysis rate of 1.2 mM (●) or 0.12 mM (○) dipalmitoyl phosphatidylcholine large unilamellar vesicles by porcine pancreatic phospholipase $A_2$ (25 μg/ml). The downward shift in the minimum lag time with increasing enzyme/lipid ratio parallels that of the lipid phase transition temperature. (Adapted from Lichtenberg et al, 1986 with permission).

profile of lipid chain-melting is superimposed on that for the transition between the states with different amide proton exchange kinetics, both determined by Fourier transform infrared spectroscopy. The two transitions are essentially coincident. The transition in tertiary structural state is found to depend on the lipid to which cytochrome *c* is bound; for other lipids it takes place wholly in the fluid state (Heimburg and Marsh, 1993). In the case of dimyristoyl phosphatidylglycerol, the transition occurs immediately on conversion to the fluid state and is controlled by the chain-melting of this lipid (Figure 22b). Because the two conformational states in Figure 22a possess different redox potentials, the shift in conformational equilibrium with change in state of the lipid, and also with change in the lipid species (Heimburg et al, 1991), will affect the electron transfer efficiency of the lipid-bound protein. As discussed earlier, the shift in the heat capacity profile suggests a stronger binding of cytochrome *c* to the gel state of dimyristoyl phosphatidylglycerol than to the fluid phase. The difference of the binding affinity, $\Delta G_P$, may contribute to the free energy required for the conformational change, and correspondingly $\Delta G_P$ may contain contributions from the structural change in the protein.

Phospholipase $A_2$ is a peripherally bound lipolytic enzyme that catalyzes the hydrolysis of phospholipids by cleavage of the ester bond of the *sn*-2 acyl chain, producing as hydrolysis products, fatty acids and lysolipids. The enzymatic activity is controlled by a number of factors, including the presence of calcium and hydrolysis products, and, depending on the lipid system, also can depend rather strongly on temperature. With membranes composed of zwitterionic phospholipids such as phosphatidylcholine, the protein is hardly active until a certain lag time has passed. After this time, a burst in activity is observed. A possible explanation for the lag time is that the aggregation kinetics of the membrane-associated enzyme are slow and only the protein aggregates are active (Biltonen, 1990). It has been found that this lag time is highly temperature dependent. In the case of pancreatic phospholipase $A_2$ binding to dipalmitoyl phosphatidylcholine bilayers, a minimum in the lag time (and a maximum in the activity) is reached close to the chain-melting phase transition temperature (see Figure 22c). At higher enzyme/lipid ratios, the minimum in lag time is shifted to lower temperatures. This parallels the aggregation behavior predicted for a peripheral protein that prefers the fluid phase over the gel phase (Figure 17 for the reverse situation). However, epifluorescence measurements on dipalmitoyl phosphatidylcholine monolayers have localized the site of action of snake venom phospholipase $A_2$ to the gel-fluid interfaces, rather than to a particular domain (Grainger et al, 1990). In this case, principles of preferential affinity similar to those for domains of lipids in a particular state could apply, but for interfacial sites considerations of enhanced lateral compressibility also may be important (see below). Unlike that of the snake venom enzyme, the binding of pancreatic phospholipase $A_2$ to zwitterionic lipids is, however, rather weak at all temperatures (Apitz-Castro et al, 1982; Jain et al, 1982). Alternative explanations for the lag time, therefore, include the generation of negatively charged fatty acids and other hydrolysis products, which increase the binding of the enzyme to the

membrane (Jain et al, 1982), and specifically the lateral phase separations induced by the hydrolysis products (Burrack et al, 1993; Jain et al, 1989). In these cases, the minimum in the lag time could be related to the ease of insertion of the protein, or conversely to the increased accessibility of the lipid substrate which arises from the enhanced lateral compressibility of the membrane in the transition region, particularly at the gel-fluid interface, as is discussed later.

A different illustration of the way in which the state of the lipids may affect the activity of peripheral proteins is afforded by the dependence of the activation of lipid-requiring enzymes on the physical form in which the activating lipid is presented. The activation of the mitochondrial enzyme D-$\beta$-hydroxybutyrate dehydrogenase by phosphatidylcholine is noncooperative with soluble monomeric lipid, but is cooperative with lipid vesicles (Cortese et al, 1987). The specific activation of the cellular regulatory enzyme protein kinase *C* by phosphatidylserine in the presence of diacylglycerol is cooperative for both micellar and bilayer lipid systems, but is more highly cooperative when the phosphatidylserine is presented in micelles (Newton, 1993). In general, the preferential interaction with a particular lipid species can be rather similar to that with a particular state of a single lipid, and can be analyzed in a similar manner. The specificity of protein kinase *C* for phosphatidylserine is an interesting case. This enzyme binds in an electrostatic manner to negatively charged lipids in general but, on binding the second messenger lipid diacylglycerol, the affinity specifically for phosphatidylserine increases greatly and to an extent that is no longer dependent on ionic strength (Orr and Newton, 1992a,b).

## FUNCTIONAL ASPECTS: INTEGRAL PROTEINS

There are many well-known examples in which the activity of integral membrane enzymes or transport systems are dependent on the state of the lipid. Among these are the $Ca^{2+}$-ATPase (Hesketh et al, 1976; Hidalgo et al, 1978; Starling et al, 1995), Na,K-ATPase (Kimelberg and Papahadjopoulos, 1974), cytochrome oxidase (Fajer et al, 1989), the erythrocyte hexose transporter (Carruthers and Melchior, 1984), and sugar transport systems in *E. coli* (Overath and Thilo, 1978). Most often, it has been found that the activity is lower in gel-phase lipids than in the corresponding fluid-phase lipids, and nonlinear Arrhenius kinetics are obtained for the temperature dependence of the activity. The form of the temperature dependence is determined by several factors, including the difference in activation enthalpies and heat capacities in the two lipid phases, and most importantly on the preferential partitioning of the protein between the coexisting lipid states (Silvius and McElhaney, 1981). In the case of sugar transport in fatty-acid supplemented auxotrophs of *E. coli*, the temperature dependence of the transport rates has been interpreted specifically in terms of different preferential phase-partitioning of the $\beta$-glucoside and $\beta$-galactoside transport systems in membranes of various lipid compositions, by comparison with the degree of lipid phase separation determined by independent means (Thilo et al, 1977). The estimated protein distribution coefficients are in the range 2–20 in favor of the

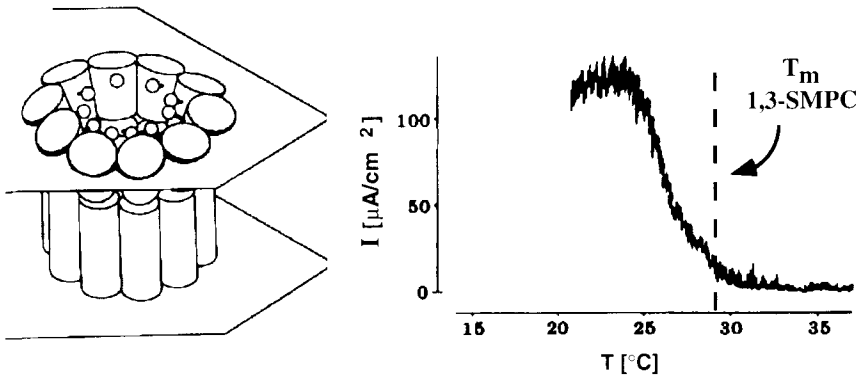


**Figure 23.** (a) Schematic structure of the alamethicin pore consisting of a complex of several single peptides. (Adapted from Fox Jr. and Richards, 1982 with permission). (b) Temperature dependence of the transmembrane current density in bilayers of 1-stearoyl-3-myristoyl phosphatidylcholine (1,3-SMPC) containing alamethicin. The vertical line indicates the gel-to-fluid phase transition temperature of 1,3-SMPC bilayers. (Adapted from Boheim et al, 1980).

fluid lipid phase. It also has been found that activity can depend on the lipid species (Bennett et al, 1978; Teft et al, 1986), which in the case of spatially separated domains of different lipid composition would again be controlled by the protein distribution.

A striking example of the effect of the lipid chain-melting transition on the activity of an ion channel is afforded by the pore-forming peptide alamethicin in planar bilayer membranes of 1-stearoyl-3-myristoyl phosphatidylcholine (see Figure 23). This unusual isomer of an asymmetric-chain phospholipid is capable of forming stable unsupported bilayers in the gel phase. The formation of ion-conducting pores by oligomerization of alamethicin monomers (Figure 23a) is very strongly concentration dependent: the conductance depends on the 9th to 10th power of the alamethicin concentration (Boheim et al, 1980). Therefore, it is to be expected that the membrane conductance would change strongly in the region of the bilayer chain-melting transition, if the degree of aggregation and hence the local concentration of alamethicin was dependent on the state of the lipid. This is exactly what is observed in Figure 23b. The current density increases from a level corresponding to only 1 pore/cm$^2$ in the fluid phase at 34°C to that corresponding to approximately $10^6$ pores/cm$^2$ in the gel phase at 24°C. Qualitatively, this parallels the aggregation behavior expected for an integral protein that exhibits a preference for the fluid phase and therefore would have a cluster profile that is the inverse of those shown in Figure 21.

*Compressibility, Protein Insertion, and Membrane Permeability*

The lateral compressibility of membranes is an important feature that may control conformational changes of embedded proteins, the insertion of proteins, peptides, presequences and other amphiphiles, as well as determining the elastic properties of the membrane (Marsh, 1996). The functional implications and possible advantages arising from the enhanced lateral compressibility of membranes in a state of lateral phase separation have long been recognized (Linden et al, 1973). Specifically in this regard, as already mentioned, the methods introduced earlier may be used also to obtain the isothermal area compressibility of membranes with the two-state model. By introducing a term dependent on the lateral pressure (or membrane tension) into the free energy, an expression for the isothermal compressibility, $\kappa_T$, can be obtained in terms of the fluctuations in the membrane area, in much the same way as was done for the heat capacity earlier (Hill, 1966):

$$\kappa_T = -\frac{1}{\langle A \rangle}\left(\frac{\partial \langle A \rangle}{\partial \pi}\right)_T = \frac{1}{\langle A \rangle}\frac{\langle A^2 \rangle - \langle A \rangle^2}{RT} \tag{36}$$

where $\pi$ is the lateral pressure (or strictly speaking surface tension) in the membrane.

Within the framework of the two-state model, the membrane area is related directly to the fraction of fluid lipids, $f$, by: $A = A_g + f\Delta A_t$, where $A_g$ and $A_l$ are the molar lipid areas in the gel and fluid phases, respectively, and $\Delta A_t = (A_l - A_g)$. The isothermal compressibility then becomes:

$$\kappa_T = \frac{\langle f^2 \rangle - \langle f \rangle^2}{RT}\frac{(\Delta A_t)^2}{A_g + \langle f \rangle \Delta A_t}. \tag{37}$$

This latter equation has strong similarities to that for the heat capacity in the two-state model that was given in Equation 29. It is, therefore, also possible to relate experimentally measured heat capacity profiles to those for the compressibility because, from Equations 29 and 37:

$$\kappa_T = \frac{\gamma^2 C_P \cdot T}{A_g + \gamma \cdot \langle \Delta H(T) \rangle} \tag{38}$$

where $\gamma = \Delta A_t / \Delta H_t$ is the proportionality constant between the transition enthalpy and the change in molar lipid area at the transition, and it will be remembered that $\Delta H(T) \approx f\Delta H_t$. For $\Delta A_t = N_A \times 18\text{Å}^2/\text{mol}$ ($\approx$37% area change), and $\Delta H_t = 8.7$ kcal/mol, the value of the proportionality constant is $\gamma = 12.5$ m$^2$/cal. The compressibility also has units of m$^2$/cal (or m/N, the units of an inverse lateral pressure).

The heat capacity profile and the corresponding temperature profile of the lateral compressibility, derived from a single series of Monte Carlo simulations for the two-state model by using Equations 29 and 37, are given in Figure 24. The parameters used are those appropriate to small unilamellar vesicles of di-

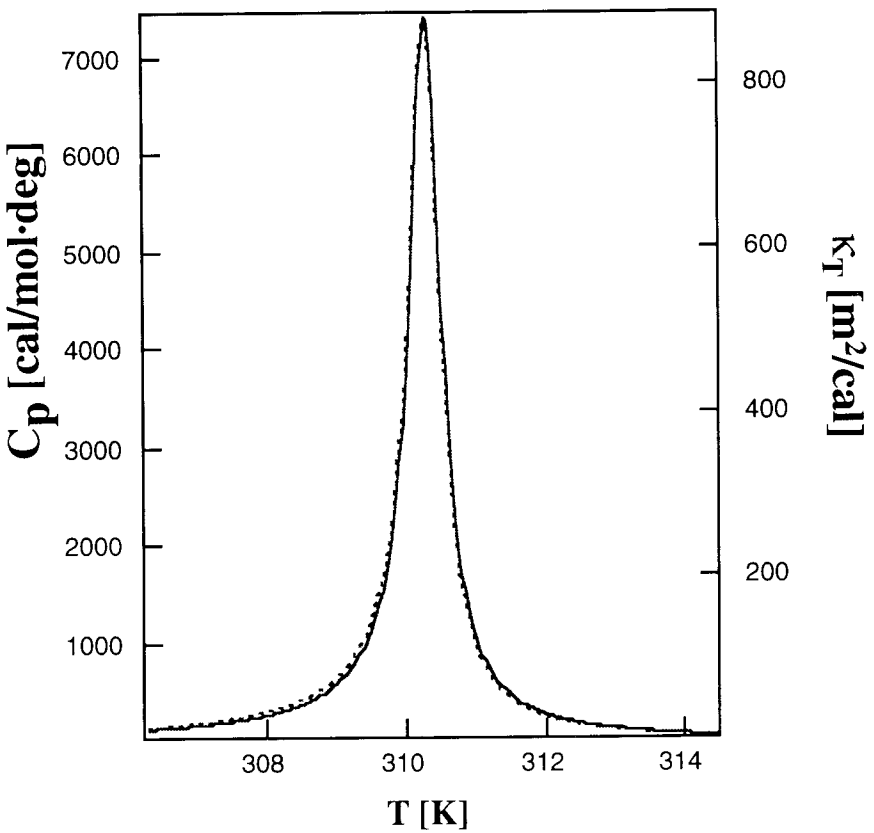


**Figure 24.** Temperature dependence of the isothermal lateral compressibility, $\kappa_T$ (dotted line) and of the heat capacity, $C_P$ (solid line) calculated from Monte Carlo simulations by using Equations 39 and 27, respectively. A 61 × 61 lipid lattice was used with $\Delta H_t = 8.7$ kcal/mol, $T_m = 310.3$ K and $\omega_{gl} = 310$ cal/mol. Surface areas were assumed to be 60 Å$^2$/lipid and 78 Å$^2$/lipid in the gel and fluid states, respectively.

palmitoyl phosphatidylcholine. The temperature dependence of the compressibility is nearly superimposable on that of the heat capacity, differing from the latter only in the temperature dependence of the mean area (divided by $T$) in the denominator of Equation 36. (The latter is introduced conventionally in defining a compressibility modulus rather than a susceptibility or response function.) The calculated heat capacity maximum in Figure 24 is $C_p^{\max} \approx 7400$ cal/mol/K, and the corresponding maximum value of the compressibility is approximately $\kappa_T^{\max} = 880$ m$^2$/cal, or 210 m/N (Equation 38). The temperature dependence of the compressibility modulus of a dimyristoyl phosphatidylcholine bilayer has been measured in the chain-melting region by pipette aspiration of giant unilamellar vesicles (Evans and Kwok, 1982). A pronounced maximum is found in the compressibility modulus at the gel-to-fluid phase transition temperature of

24°C and the compressibility decreases steeply away from the transition region on going to either the gel or fluid phase, as is predicted by the two-state model in Figure 24. The compressibility modulus has a value of $\kappa_T^{\max} = 30$–$50$ m/N at the phase transition temperature, and values of $\kappa_T \approx 1$ m/N at 8°C and $\approx 7$ m/N at 30°C in the gel and fluid states, respectively. The higher value at 30°C than at 8°C corresponds to the intrinsic lateral compressibility of the fluid state that is not included in the two-state model.

The enhanced lateral compressibility, and accompanying fluctuations in the lipid area (Equation 36) that occur in the gel-fluid coexistence region promote the formation of defects and transient pores in the lipid matrix. The nucleation site for such defects is the interfacial region between the gel and fluid domains. This is the site of locally higher free energy and the point at which the conversion between gel and fluid states, which is the origin of the high compressibility, primarily takes place (Figure 10). One of the consequences of this can be, depending on solute size (Van Hoogevest et al, 1984), an increased permeability of the membrane to polar solutes, which otherwise have an intrinsically low permeability in the isolated lipid states. The permeability to alkali ions and the ionic conductivity of lipid bilayers, for instance, have been found to have a maximum in the region of the gel-fluid phase transition (Blok et al, 1975; Papahadjopoulos et al, 1973; Wu and McConnell, 1973).

The temperature dependence of the permeability of monodisperse, small unilamellar vesicles of dimyristoyl phosphatidylcholine to a small spin-labeled cation (Tempocholine) is given in Figure 25. Data are presented for both uptake and release, in which the latter corresponds to the somewhat lower of the biphasic transport rates that is obtained at longer times (Marsh et al, 1976). The rates of both permeability processes display a maximum at the phase transition region, which in this case is rather broad because of the low cooperativity of the phase transition in small unilamellar lipid vesicles (Marsh et al, 1977). The permeability profiles are compared with calculations of the lateral compressibility and the fraction of interfacial lipids, using for analytical simplicity a one-dimensional two-state Ising model rather than the rigorous Monte Carlo simulations for a two-dimensional system that were given above. The compressibility is calculated from Equations 23 and 37. The degree of cooperativity of the transition ($\sigma_L = 4.10^{-3}$) is determined from independent measurements of the degree of transition. As expected, both the compressibility and the fraction of interfacial lipids display a maximum at the center of the phase transition, but the temperature profile for the compressibility is narrower than that for the fraction of interfacial lipids. The permeabilities on the low temperature side of the transition correspond more closely to the compressibility and those on the high temperature side to the fraction of interfacial lipids. This asymmetry possibly corresponds in part to a higher intrinsic permeability for the defects at the interfacial regions in a predominantly fluid environment. The compressibility calculated at the center of the transition is $\kappa_T^{\max} \approx 20$ m/N, which is comparable to that measured experimentally for dimyristoyl phosphatidylcholine bilayers, although the cooperativity is lower for small vesicles.

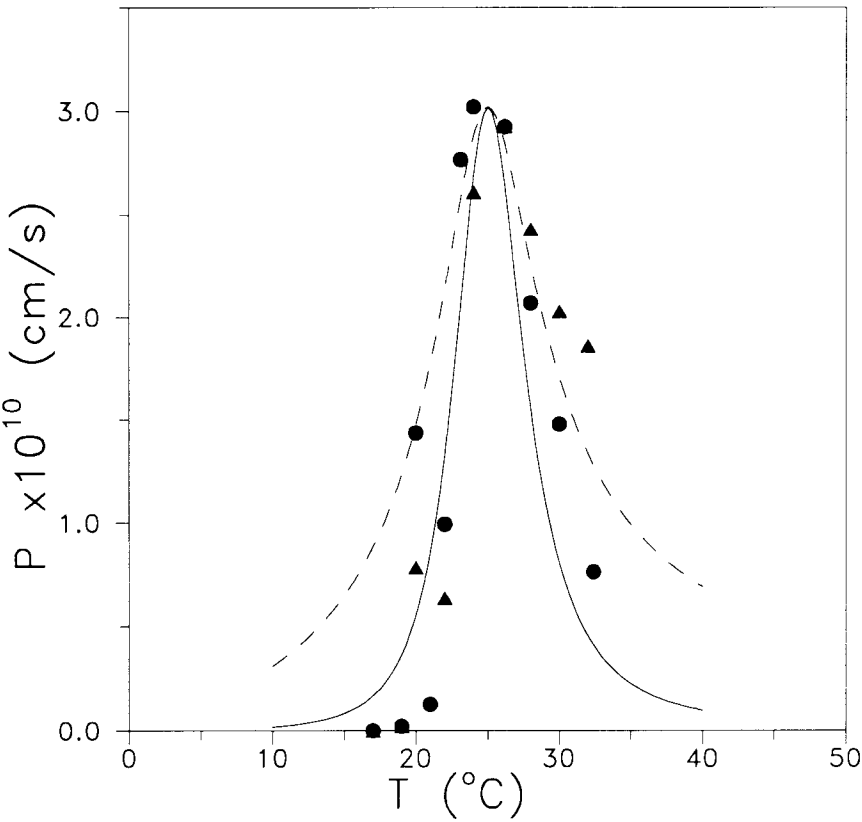


**Figure 25.** Temperature dependence of the permeability, $P$, of small unilamellar vesicles of dimyristoyl phosphatidylcholine to the cation, Tempocholine$^+$. Permeabilities were determined from the initial rate of uptake (●) and from release over a longer timescale (▲). For the latter, the ordinate is to be multiplied by a factor of 0.23. (Initial rates of release gave similar permeabilities to those from uptake.) The lateral compressibility (solid line) and fraction of interfacial lipids (dashed line) were calculated for a one-dimensional Ising model as described in the text. The maximum compressibility is 19 m/N and the maximum fraction of interfacial lipids is 3%. (Adapted from Marsh et al, 1976 with permission).

A range of other experiments have also indicated different aspects of lipid membrane function for which a maximum in activity is exhibited at the chain-melting transition or in regions of gel-fluid lateral phase separation. A maximum in the partitioning of amphiphiles, such as the fluorescence probe anilinonapthalene sulphonic acid (Jacobsen and Papahadjopoulos, 1976; Tsong, 1975) and lysolipids (Harlos et al, 1977), into lipid vesicles has been demonstrated at the gel-to-fluid phase transition. The incorporation of the bacteriophage M13 coat protein into synthetic lipid membranes is maximal (and complete) at the chain-melting transition, and only in the transition region is the incorporated coat protein able to adopt the correct transmembrane orientation (Wickner, 1976).

A discontinuous increase in sugar transport activity with decreasing temperature has been observed in fatty-acid supplemented auxotrophs of *E. coli* on entering the lateral phase separation region of the membrane lipids from the fluid phase (Linden et al, 1973). As mentioned previously, the lipolytic activity of pancreatic phospholipase $A_2$ is maximum at the bilayer phase transition of the lipid substrate, and this extends also to the gel-fluid coexistence region of lipid mixtures (Op den Kamp et al, 1975). Experiments with monolayers have located the site of action of snake venom phospholipase $A_2$ at the interfacial regions between coexisting gel and fluid domains, i.e., exactly in those regions where the enhanced lateral compressibility is expressed (Grainger et al, 1990). Measurements of trapped volume have shown that the extent of fusion of freshly sonicated dipalmitoyl phosphatidylcholine vesicles, essentially an annealing process, is maximal at the phase transition (Marsh and Watts, 1981). All these results suggest that the high lateral compressibility of lipid bilayers in their regions of gel-fluid coexistence, and the accompanying fluctuations and creation of transient membrane defects, facilitates the insertion of membrane molecules and other amphiphiles and enhances the function of surface-active enzymes.

*Propagation of Compressional Waves*

A further feature of the elastic properties of surfaces is the possibility for propagation of mechanical distortions through the planar membrane which could be considered as a two-dimensional compression wave. This might serve as a possible means of communication between membrane proteins, the conformational changes of which are sensitive to, and could generate, propagating changes in the membrane lateral pressure. A local change in lipid surface density will lead to a local increase in temperature because the work of compression will convert to an equivalent thermal energy. If the distortion is so short that this thermal energy cannot dissipate by diffusion, the local compression is described by the adiabatic compressibility, $\kappa_S$, rather than by the isothermal compressibility, $\kappa_T$. The adiabatic compressibility depends on the heat capacity and the isothermal compressibility, and for simplicity we assume that the adiabatic and the isothermal compressibility have approximately the same temperature dependence and comparable quantitative values. The bulk compressibility of dipalmitoyl phosphatidylcholine bilayers deduced from ultrasonic velocity measurements (Mitaku et al, 1978) is found to be a factor of approximately 2.5 times smaller than that obtained from static isothermal measurements (Liu and Kay, 1977; Marsh, 1990). The velocity, $c_0$, of the compression wave, at frequencies well below the rates of processes contributing to the velocity dispersion, is related to the adiabatic area compressibility by an inverse square root dependence:

$$\frac{1}{c_0^2} = \left(\frac{\partial \rho_A}{\partial \pi}\right)_S = -\frac{\rho_A}{A}\left(\frac{\partial A}{\partial \pi}\right)_S = \rho_A \cdot \kappa_S \tag{39}$$

where $\rho_A$ is the surface density. From the results of the previous section, it is therefore expected that the speed of sound in a membrane is slowest at the transition mid-point and increases strongly outside the transition region. Such slowing-down effects have been found experimentally for ultrasonic velocity measurements in bulk membrane dispersions. An abrupt decrease in ultrasonic velocity in the bilayers by approximately 270 m/s has been found at the phase transition of dipalmitoyl phosphatidylcholine (Mitaku et al, 1978). In this latter situation, however, it is the three-dimensional propagation and the volume compressibility that are involved.

The density $\rho_A$ used in Equation 39 is the mass per unit area, which is approximately $4.4 \cdot 10^{-3}$ g/m$^2$ (assuming an area of 60 Å$^2$ per lipid and a molar mass of 800 g/mol). Using the isothermal compressibility, instead of the adiabatic compressibility, yields a velocity for the compression wave at the lipid transition point of approximately 33 m/s. (Correction to the adiabatic compressibility, by scaling according to the ratio of the bulk values given above, yields approximately 52 m/s.) The velocity is slower for more cooperative transitions and faster for less cooperative transitions, and increases steeply outside the transition range. In large membranes, this propagation could, in principle, play a role in signal transduction within the membrane plane. In charged membranes, these signals might propagate not only changes in temperature and density, but also changes in electrostatic surface potential. As discussed earlier, changes of surface potential play a role in binding affinities and in structural equilibria of the bound proteins. In general, therefore, it is possible that structural changes in the proteins could reciprocally trigger the propagation of electrostatic and density waves, resulting in a communication between membrane proteins.

## Conclusions

This chapter has been concerned with the thermodynamics of interactions of lipid membranes with, principally, peripheral proteins. First, the binding has been analyzed, which gives information on the free energy of interaction, in which electrostatics plays a very major role. Additionally, it has been shown that binding isotherms can give information on the interactions between the surface-bound proteins, on the interactions between the lipids to which they are bound, and on their redistribution in response to the binding of proteins. The second aspect considered has been the preferential interaction of membrane proteins with lipids in different physical states at the chain-melting transition, and by implication more generally, in regions of lateral lipid phase separation. The thermodynamics of lipid chain-melting has been shown to reflect also that of protein binding and constitutes a viable alternative method for studying the difference in energetics of protein binding to lipid membranes in different states. By combining experimental thermodynamic measurements with theoretical Monte Carlo simulations, information has been obtained on the distribution of proteins

at the surface of the membrane, or within the membrane (in the case of integral proteins). These protein distributions are important not only in cases in which function specifically requires aggregation or clustering of proteins, but also quite generally in determining possible structural interactions, the likelihood of encounters, and the spatial relations between the different membrane components. Finally, the coupling between thermodynamic fluctuations and structural fluctuations linked to changes in membrane area has been addressed, leading to consideration of the possible functional consequences of enhanced membrane compressibility.

It should be noted that, although a considerable part of this chapter has concentrated on gel-to-fluid lipid phase transitions, the principal results are generally applicable to membranes with any form of coexistence of lipid states, in particular those arising from a heterogeneity in lipid composition or from specific binding of divalent ions. Relevant thermodynamic parameters in all cases are the heat capacities, enthalpies, interfacial energies between lipids of different type, and the differential binding free energies. These general results, therefore, may form some physical rationale for the complex chemical composition of the lipids in biological membranes.

## REFERENCES


Albon N, Sturtevant JM (1978): Nature of the gel to liquid crystal transition of synthetic phosphatidylcholines. *Proc Natl Acad Sci USA* 75:2258–2260

Apitz-Castro R, Jain MK, de Haas GH (1982): Origin of the latency phase during the action of phospholipase $A_2$ on unmodified phosphatidylcholine vesicles. *Biochim Biophys Acta* 688:349–356

Aveyard R, Haydon DA (1973): *An Introduction to the Principles of Surface Chemistry*. Cambridge: Cambridge University Press

Bennett JP, Smith GA, Houslay MD, Hesketh TR, Metcalfe JC, Warren GB (1978): The phospholipid headgroup specificity of an ATP-dependent calcium pump. *Biochim Biophys Acta* 513:310–320

Biltonen RL (1990): A statistical-thermodynamic view of cooperative structural changes in phospholipid bilayer membranes: Their potential role in biological function. *J Chem Thermody* 22:1–19

Blok MC, van der Neut-Kok ECM, van Deenen LLM, de Gier J (1975): The effect of chainlength and lipid phase transitions on the selective permeability properties of liposomes. *Biochim Biophys Acta* 406:187–196

Boggs JM, Clement IR, Moscarello MA (1980): Similar effect of proteolipid apoproteins from human myelin (lipophilin) and bovine white matter on the lipid phase transition. *Biochim Biophys Acta* 601:134–151

Boggs JM, Rangaraj G, Kostry KM (1988): Photolabeling of myelin basic protein in lipid vesicles with the hydrophobic reagent 3-(trifluoromethyl)-3-(*m*-[$^{125}$I]iodophenyl) diazirine. *Biochim Biophys Acta* 937:1–9

Boheim G, Hanke W, Eibl H (1980): Lipid phase transition in a planar bilayer and its effect on carrier- and pore-mediated transport. *Proc Natl Acad Sci USA* 77:3403–3407

Burack WR, Yuan Q, Biltonen RL (1993): Role of lateral phase separation in the modulation of phospholipase $A_2$ activity. *Biochemistry* 31:583–589

Cantor CR, Schimmel PR (1980): *Biophysical Chemistry, Vol. 3*.New York: Freeman

Carruthers A, Melchior DL (1984): Human erythrocyte hexose transporter activity is governed by bilayer lipid composition in reconstituted vesicles. *Biochemistry* 23:6901–6911

Cevc G, Marsh D (1987): *Phospholipid Bilayers. Physical Principles and Models*. New York: Wiley-Interscience

Cevc G, Watts A, Marsh D (1981): Titration of the phase transition of phosphatidylserine bilayer membranes. Effects of pH, surface electrostatics, ion binding and head-group hydration. *Biochemistry* 20:4955–4965

Cevc G, Watts A, Marsh D (1980): Non-electrostatic contribution to the titration of the ordered-fluid phase transition of phosphatidylglycerol bilayers. *FEBS Lett* 120:267–270

Cheddar G, Tollin G (1994): Comparison of electron transfer kinetics between redox proteins free in solution and electrostatically complexed to a lipid bilayer membrane. *Arch Biochem Biophys* 310:392–396

Chen YS, Hubbell WL (1973): Temperature- and light-dependent structural changes in rhodopsin-lipid membranes. *Exp Eye Res* 17:517–532

Cortese JD, Fleischer S (1987): Noncooperative vs. cooperative reactivation of D-$\beta$-hydroxybutyrate dehydrogenase: Multiple equilibria for lecithin binding are determined by the physical state (soluble vs. bilayer) and composition of the phospholipids. *Biochemistry* 26:5283–5293

Cutsforth GA, Whitaker RN, Hermans J, Lentz BR (1989): A new model to describe extrinsic protein binding to phospholipid membranes of varying composition: Application to human coagulation proteins. *Biochemistry* 28:7453–7461

Daum G (1985): Lipids of mitochondria. *Biochim Biophys Acta* 822:1–42

Dickerson RE, Takano T, Eisenberg D, Kallai OB, Samson L, Cooper A, Margoliash EJ (1971): Ferricytochrome *c* 1. General features of the horse and bonito proteins at 2.8 Å resolution. *J Biol Chem* 246:1511–1535

Evans EA, Kwok R (1982): Mechanical calorimetry of large dimyristoyl phosphatidylcholine vesicles in the phase transition region. *Biochemistry* 21:4874–4879

Fajer P, Knowles PFK, Marsh D (1989): Rotational motion of yeast cytochrome oxidase in phosphatidylcholine complexes studied by saturation-transfer electron spin resonance. *Biochemistry* 28:5634–5643

Ferrenberg AM, Swendsen RH (1988): New Monte Carlo technique for studying phase transitions. *Phys Rev Lett* 61:2635–2638

Fox RO, Jr., Richards FM (1982): A voltage-gated ion channel model inferred from the crystal structure of alamethicin at 1.5-A resolution. *Nature* 30:325–330

Freire E, Markello T, Rigell C, Holloway PW (1983): Calorimetric and fluorescence characterization of interactions between cytochrome $b_5$ and phosphatidylcholine bilayers. *Biochemistry* 22:1675–1680

Görrisen H, Marsh D, Rietveld A, de Kruijff B (1986): Apocytochrome *c* binding to negatively charged lipid dispersions studied by spin-label electron spin resonance. *Biochemistry* 25:2904–2910

Grainger DW, Reichert A, Ringsdorf H, Salesse C (1990): Hydrolytic action of phospholipase $A_2$ in monolayers in the phase transition region: Direct observation of enzyme domain formation using fluorescence microscopy. *Biochim Biophys Acta* 1023:365–379

Grant CWM, McConnell HM (1974): Glycophorin in lipid bilayers. *Proc Natl Acad Sci USA* 71:4653–4657

Harlos K, Vaz WLC, Kovatchev S (1977): Effect of desoxylysolecithins on dimyristoyllecithin vesicles. Influence of the lipid phase transition. *FEBS Lett* 77:7–10

Haydon DA, Taylor FH (1960): On adsorption at the oil/water interface and the calculation of electrical potentials in the aqueous surface phase. I. Neutral molecules and a simplified treatment for ions. *Phil Trans Roy Soc* A 252:225–248

Heimburg T, Biltonen RL (1996): A Monte-Carlo simulation study of protein-induced heat capacity changes and lipid-induced protein clustering. *Biophys J* 70:84–96

Heimburg T, Biltonen RL (1994): Thermotropic behavior of dimyristoylphosphatidylglycerol and its interaction with cytochrome *c*. *Biochemistry* 33:9477–9488

Heimburg T, Marsh D (1995): Protein surface-distribution and protein-protein interactions in the binding of peripheral proteins to charged lipid membranes. *Biophys J* 68:536–546

Heimburg T, Marsh D (1993): Investigation of secondary and tertiary structural changes of cytochrome *c* in complexes with anionic lipids using amide hydrogen exchange measurements: An FTIR study. *Biophys J* 65:2408–2417

Heimburg T, Hildebrandt P, Marsh D (1991): Cytochrome *c*-lipid interactions studied by resonance Raman and $^{31}$P-NMR spectroscopy. Correlation between the conformational changes of the protein and the lipid bilayer. *Biochemistry* 30:9084–9089

Hesketh TR, Smith GA, Houslay MD, McGill KA, Birdsall, NJM, Metcalfe JC, Warren GB (1976): Annular lipids determine the ATPase activity of a calcium transport protein complexed with dipalmitoyllecithin. *Biochemistry* 15:4145–4151

Hidalgo C, Thomas DD, Ikemoto N (1978): Effect of the lipid environment on protein motion and enzymatic activity of the sarcoplasmic reticulum calcium ATPase. *J Biol Chem* 253:6879–6887

Hildebrandt P, Stockburger M (1989a): Cytochrome *c* at charged interfaces. 1. Conformational and redox equilibria at the electrode/electrolyte interface probed by surface-enhanced Raman spectroscopy. *Biochemistry* 28:6710–6721

Hildebrandt P, Stockburger M (1989b): Cytochrome *c* at charged interfaces. 2. Complexes with negatively charged macromolecular systems studied by resonance Raman spectroscopy. *Biochemistry* 28:6722–6728

Hildebrandt P, Heimburg T, Marsh D (1990): Quantitative conformational analysis of cytochrome *c* bound to phospholipid vesicles studied by resonance Raman spectroscopy. *Eur Biophys J* 18:193–201

Hill TL (1960): *An Introduction to Statistical Thermodynamics*. New York: Dover

Hill TL (1946): Statistical mechanics of multimolecular absorption. II. Localized and mobile adsorption and absorption. *J Chem Phys* 14:441–453

Huang J, Swanson JE, Dibble ARG, Hinderliter AK, Feigenson GW (1993): Nonideal mixing of phosphatidylserine and phosphatidylcholine in the fluid lamellar phase. *Biophys J* 64:413–425

Jacobson K, Papahadjopoulos D (1976): Effect of phase transition on the binding of 1-anilino-8-naphthalenesulfonate to phospholipid membranes. *Biophys J* 16:549–560

Jähnig F (1976): Electrostatic free energy and shift of the phase transition for charged lipid membranes. *Biophys Chem* 4:309–318

Jain MK, Vaz WLC (1987): Dehydration of the lipid-protein microinterface on binding phospholipase $A_2$ to lipid bilayers. *Biochim Biophys Acta* 905:1–8

Jain MK, Egmond MR, Verheij H, Apitz-Castro R, Dijkman R, de Haas GH (1982): Interaction of phospholipase $A_2$ and phospholipid bilayers. *Biochim Biophys Acta* 688:341–348

Jain MK, Yu B-Z, Kozubek A (1989): Binding of phospholipase $A_2$ to zwitterionic bilayers is promoted by lateral segregation of anionic amphiphiles. *Biochim Biophys Acta* 980:23–32

Kimelberg HK, Papahadjopoulos D (1974): Effects of phospholipid acyl chain fluidity, phase transitions and cholesterol on $(Na^+ + K^+)$-stimulated adenosine triphosphatase. *J Biol Chem* 249:1071–1080

Kleeman W, McConnell HM (1976): Interactions of proteins and cholesterol with lipids in bilayer membranes. *Biochim Biophys Acta* 419:206–222

Kleeman W, McConnell HM (1974): Lateral phase separations in Escherichia coli membranes. *Biochim Biophys Acta* 345:220–230

Lee J, Kosterlitz JM (1991): Finite-size scaling and Monte Carlo simulations of first-order phase transitions. *Phys Rev* B 43:3265–3277

Lichtenberg D, Romero G, Menashe M, Biltonen RL (1986): Hydrolysis of dipalmitoyl phosphatidylcholine large unilamellar vesicles by porcine pancreatic phospholipase $A_2$. *J Biol Chem* 261:5334–5340

Linden C, Wright K, McConnell HM, Fox CF (1973): Phase separations and glucoside uptake in *E. coli* fatty acid auxotrophs. *Proc Natl Acad Sci USA* 70:2271–2275

Liu NI, Kay RL (1977): Redetermination of the pressure dependence of the lipid bilayer phase transition. *Biochemistry* 16:3484–3486

London Y, Demel RA, Guerts van Kessel WSM, Vossenberg FGA, van Deenen LLM (1979): The protection of $A_1$ myelin basic protein against the action of proteolytic enzymes after injection of the protein with lipids at the air-water interface. *Biochim Biophys Acta* 311:520–530

Marsh D (1996): Lateral pressure in membranes. *Biochim Biophys Acta*: in press

Marsh D (1995a): Specificity of lipid-protein interactions. In: *Biomembranes*, Vol. 1, Lee AG, ed. Greenwich, CT: JAI Press

Marsh D (1995b): Lipid-protein interactions and heterogeneous lipid distribution in membranes. *Mol Memb Biol* 12:59–64

Marsh D (1990): *Handbook of Lipid Bilayers*. Boca Raton, FL: CRC Press

Marsh D (1985): ESR spin label studies of lipid-protein interactions. In: *Progress in Protein-Lipid Interactions*, Vol. 1, Watts A, de Pont JJHHM, eds. Amsterdam: Elsevier

Marsh D, Watts A (1981): ESR spin label studies. In: *Liposomes: from Physical Structure to Therapeutic Applications*, Knight CG, ed. Amsterdam: Elsevier/North-Holland Biomedical Press

Marsh D, Watts A, Knowles PF (1977): Cooperativity of the phase transition in single- and multibilayer lipid vesicles. *Biochim Biophys Acta* 465:500–514

Marsh D, Watts A, Knowles PF (1976): Permeability of Tempo-choline into dimyristoyl phosphatidylcholine vesicles at the phase transition. *Biochemistry* 15:3570–3578

Mitaku S, Ikegami A, Sakanishi A (1978): Ultrasonic studies of lipid bilayer. Phase transition in synthethic phosphatidylcholine liposomes. *Biophys Chem* 8:295–304

Morrow MR, Davis JH, Sharom FJ, Lamb MP (1986): Studies of the interaction of human erythrocyte band 3 with membrane lipids using deuterium nuclear magnetic resonance and differential scanning calorimetry. *Biochim Biophys Acta* 858:13–20

Mouritsen OG, Biltonen RL (1992): Protein-lipid interactions and membrane heterogeneity. In: *Protein-Lipid Interactions. New Comprehensive Biochemistry*, Vol. 25, Watts A, ed. Amsterdam: Elsevier

Muga A, Mantsch HH, Surewicz WK (1991): Membrane binding induces destabilization of cytochrome *c* structure. *Biochemistry* 30:7219–7224

Mühlebach T, Cherry RJ (1985): Rotational diffusion and self-association of band 3 in reconstituted lipid vesicles. *Biochemistry* 24:975–983

Newton AC (1993): Interaction of proteins with lipid headgroups: Lessons from protein kinase C. *Annu Rev Biophys Biomol Struct* 22:1–25

Op den Kamp JAF, Kauerz MTh, van Deenen LLM (1975): Action of pancreatic phospholipase $A_2$ on phosphatidylcholine bilayers in different physical states. *Biochim Biophys Acta* 406:169–177

Orr JW, Newton AC (1992a): Interaction of protein kinase C with phosphatidylserine 1. Cooperativity in lipid binding. *Biochemistry* 31:4661–4667

Orr JW, Newton AC (1992b): Interaction of protein kinase C with phosphatidylserine. 2. Specificity and regulation. *Biochemistry* 31:4667–4673

Overath P, Thilo L (1978): Structural and functional aspects of biological membranes revealed by lipid phase transitions. In: *Biochemistry of Cell Walls and Membranes II*, Metcalfe JC, ed. London: Butterworth and University Park Press

Papahadjopoulos D, Jacobson K, Nir S, Isac T (1973): Phase transitions in phospholipid vesicles. Fluorescence polarization and permeability experiments concerning the effects of temperature and cholesterol. *Biochim Biophys Acta* 311:330–348

Ramsay G, Prabhu R, Freire E (1986): Direct measurement of the energetics of association between myelin basic protein and phosphatidylserine vesicles. *Biochemistry* 25:2265–2270

Ryba NJP, Marsh D (1992): Protein rotational diffusion and lipid/protein interactions in recombinants of bovine rhodopsin with saturated diacyl-phosphatidylcholines of different chainlengths studied by conventional and saturation-transfer electron spin resonance. *Biochemistry* 31:7511–7518

Sankaram MB, Marsh D (1993): Protein-lipid interactions with peripheral membrane proteins. In: *Protein-Lipid Interactions. New Comprehensive Biochemistry*, Vol. 25, Watts A, ed. Amsterdam: Elsevier

Sankaram MB, Brophy PJ, Jordi W, Marsh D (1990): Fatty acid pH titration and the selectivity of interaction with extrinsic proteins in dimyristoylphosphatidylglycerol dispersions. Spin label ESR studies. *Biochim Biophys Acta* 1021:63–69

Sankaram MB, Brophy PJ, Marsh D (1989a): Spin-label ESR studies on the interaction of bovine spinal cord myelin basic protein with dimyristoylphosphatidylglycerol dispersions. *Biochemistry* 28:9685–9691

Sankaram MB, de Kruijff B, Marsh D (1989b): Selectivity of interaction of spin-labelled lipids with peripheral proteins bound to dimyristoyl phosphatidylglycerol bilayers, as determined by ESR spectroscopy. *Biochim Biophys Acta* 986:315–320

Silvius JR, McElhaney RN (1991): Non-linear Arrhenius plots and the analysis of reaction and motional rates in membranes. *J Theoret Biol* 88:135–152

Starling AP, East JM, Lee AG (1995): Effects of gel phase phospholipid on $Ca^{2+}$-ATPase. *Biochemistry* 34:3084–3091

Sugar IP, Biltonen RL, Mitchard N (1994): Monte Carlo simulations of membranes: Phase transition of small unilamellar dipalmitoylphosphatidylcholine vesicles. *Methods Enzymol* 240:569–593

Surewicz WA, Moscarello MA, Mantsch HH (1987): Fourier transform infrared spectroscopic investigation of the interaction between myelin basic protein and dimyristoylphosphatidylglycerol bilayers. *Biochemistry* 26:3881–3886

Tanford C (1955): The electrostatic free energy of globular protein ions in aqueous solution. *J Phys Chem* 59:788–793

Teft RC Jr, Carruthers A, Melchior DL (1986): Reconstituted human erythrocyte sugar transporter activity is determined by bilayer lipid headgroups. *Biochemistry* 25:3709–3718

Thilo L, Träuble H, Overath P (1977): Mechanistic interpretation of the influence of lipid phase transitions on transport functions. *Biochemistry* 16:1283–1290

Tsong TY (1975): Effect of a phase transition on the kinetics of dye transport in phospholipid bilayer structures. *Biochemistry* 14:5409–5414

Van Hoogevest P, de Gier J, de Kruijff B (1984): Determination of the size of the packing defects in dimyristoyl phosphatidylcholine bilayers, present at the phase transition temperature. *FEBS Lett* 171:160–164

Wickner W (1976): Asymmetric orientation of phage M13 coat protein in *Escherichia coli* cytoplasmic membranes and in synthetic lipid vesicles. *Proc Natl Acad Sci USA* 73:1159–1163

Wu SH, McConnell HM (1973): Lateral phase separations and perpendicular transport in membranes. *Biochem Biophys Res Commun* 55:484–491

Zimm BH, Bragg JK (1959): Theory of the phase transition between helix and random coil in polypeptide chains. *J Chem Phys* 31:526–535